Title

NEF-Induced HIV-Associated Nephropathy Through HCK/LYN Tyrosine Kinases.

Journal

The Journal of medical research, 193(6)

Authors

Hu, Chunyan
Priceputu, Elena
Cool, Marc
et al.

Publication Date

2023-06-01

DOI

10.1016/j.ajpath.2023.02.006

Peer reviewed

The American Journal of Pathology, Vol. 193, No. 6, June 2023

ELSEVIER

The American Journal of
PATHOLOGY

ajp.amjpathol.org

CARDIOVASCULAR, PULMONARY, AND RENAL PATHOLOGY

NEF-Induced HIV-Associated Nephropathy Through HCK/LYN Tyrosine Kinases

Chunyan Hu,* Elena Priceputu,* Marc Cool,* Pavel Chrobak,* Nathalie Bouchard,* Clara Forestier,* Clifford A. Lowell,† Serge Bénichou,‡ Zaher Hanna,*§¶ Virginie Royal,‖ and Paul Jolicoeur**¶

From the Laboratory of Molecular Biology, Clinical Research Institute of Montreal, Montreal, Quebec, Canada; the Department of Laboratory Medicine,† University of California, San Francisco, California; Insitut Cochin,‡ Centre National de la Recherche Scientifique UMR8104, Université Paris Descartes and INSERM U1016, Paris, France; the Departments of Medicine,§ Pathology and Cellular Biology,‖ and Microbiology/Immunology,** University of Montreal, Montreal, Quebec, Canada; and the Division of Experimental Medicine,¶ McGill University, Montreal, Quebec, Canada*

Accepted for publication February 15, 2023.

Address correspondence to Paul Jolicoeur, M.D., Ph.D., Clinical Research Institute of Montréal, 110 Pine Ave. W., Montréal, Québec H2W 1R7, Canada. E-mail: paul.jolicoeur@ircm.qc.ca.

HIV-1—associated nephropathy (HIVAN) is a severe complication of HIV-1 infection. To gain insight into the pathogenesis of kidney disease in the setting of HIV, a transgenic (Tg) mouse model [CD4C/HIV-negative regulator factor (Nef)] was used in which HIV-1 *nef* expression is under control of regulatory sequences (CD4C) of the human *CD4* gene, thus allowing expression in target cells of the virus. These Tg mice develop a collapsing focal segmental glomerulosclerosis associated with microcystic dilatation, similar to human HIVAN. To identify kidney cells permissive to the CD4C promoter, CD4C reporter Tg lines were used. They showed preferential expression in glomeruli, mainly in mesangial cells. Breeding CD4C/HIV Tg mice on 10 different mouse backgrounds showed that HIVAN was modulated by host genetic factors. Studies of gene-deficient Tg mice revealed that the presence of B and T cells and that of several genes was dispensable for the development of HIVAN: those involved in apoptosis (*Trp53*, *Tnfsf10*, *Tnf*, *Tnfrsf1b*, and *Bax*), in immune cell recruitment (*Ccl3*, *Ccl2*, *Ccr2*, *Ccr5*, and *Cx3cr1*), in nitric oxide (NO) formation (*Nos3* and *Nos2*), or in cell signaling (*Fyn*, *Lck*, and *Hck/Fgr*). However, deletion of *Src* partially and that of *Hck/Lyn* largely abrogated its development. These data suggest that Nef expression in mesangial cells through hematopoietic cell kinase (Hck)/Lck/Yes novel tyrosine kinase (Lyn) represents important cellular and molecular events for the development of HIVAN in these Tg mice. *(Am J Pathol 2023, 193: 702—724; https://doi.org/10.1016/j.ajpath.2023.02.006)*

HIV-1—associated nephropathy (HIVAN) is one of the numerous manifestations of the HIV-1[1,2] and SIV[3—5] infection. Its main pathologic lesions are collapsing focal segmental glomerulosclerosis (FSGS), tubulo-interstitial infiltration, and microcystic tubular dilatation.[1] The glomerular disease is associated with mesangial cell hyperplasia, loss of podocyte-specific markers,[6,7] and proliferation of glomerular cells considered to represent podocytes by some investigators.[1,6,7] These observations led to the suggestion that HIVAN results from the action of *HIV-1* gene products in podocytes.[8,9] However, other experiments have shown that proliferating cells in human HIVAN glomeruli represent parietal cells and not podocytes.[10,11] The identity of the renal target cells infected with HIV in human or SIV in primates has also remained controversial, with some groups reporting no evidence of infection,[3,12,13] whereas others finding viral footprints in podocytes and parietal and tubular cells.[8,14—19] As illustrated by these discordant reports, the pathogenesis of HIVAN in human is not well understood.

As a consequence, studies on HIVAN pathogenesis have relied on the use of animal models or cultured kidney cells *in vitro*. The Tg26 transgenic (Tg) HIVAN model has provided interesting information, in particular highlighting the need for HIV expression in kidney parenchyma.[20] However, the widespread expression of HIV RNA in

Supported by Canadian Institutes of Health Research grants MT10313 and HOP98829, the Kidney Foundation of Canada grant KFOC150011, and the National Heart, Lung, and Blood Institute (NIH) grant HL-083470 (P.J.).

Disclosures: None declared.

C.H. and E.P. contributed equally to this work.

https://doi.org/10.1016/j.ajpath.2023.02.006

Tg26 renal parenchyma[16,20,21] has made difficult the task of assigning specific pathologic lesions to *HIV* gene expression in specific kidney cell subsets. Nevertheless, podocytes from Tg26 mice[21–23] or *nef*-transduced podocytes cultured *in vitro*[9,24] showed enhanced proliferation, reinforcing the idea that HIVAN results from negative regulator factor (Nef) action in podocytes. However, other experiments revealed that a more restricted expression of Nef in Tg podocytes was not sufficient to induce the full spectrum of HIVAN,[25,26] challenging a model of disease initiated by Nef-expressing podocytes.

A different model of AIDS, the CD4C/HIV Tg mice,[27,28] has been used to study the pathogenesis of kidney disease in the setting of HIV. These Tg mice show several immune manifestations of HIV-1 infection, such as specific loss of $CD4^+$ T cells as well as lung,[27,28] heart,[29] and bone[30] diseases and severe kidney disease.[27,28] Nef was found to be necessary and sufficient to induce all these phenotypes, including kidney disease.[28,31] In these Tg mice, HIV-1 is expressed faithfully, in the natural target cells of HIV-1, through the regulatory sequences (CD4C) of the human *CD4* gene [namely, in thymic and peripheral $CD4^+$ T cells and myeloid-derived cells (tissue macrophages, alveolar macrophages, Kupffer cells, microglial cells, dendritic cells, and osteoclasts)].[27,28,30,32,33]

Kidney disease of CD4C/HIV Tg mice can not be transferred by transplantation of Tg hematopoietic cells[34] and still develops in the absence of $CD4^+$ T cells.[35] Also, restricted expression of *nef* in Tg $CD4^+$ T cells, macrophages, or dendritic cells did not cause kidney disease.[34] In addition, several *nef* mutants[36–38] or alleles,[39] individually expressed in Tg mice with the CD4C promoter, indicated that many of them, including Nef-A_{72}xxA_{75}xxQ_{78},[31] which prevents Nef/hematopoietic cell kinase (Hck) interaction, did not induce kidney disease. In fact, this analysis of *nef* mutants and alleles made it possible to determine that kidney disease and T-cell phenotypes segregated independently. These results suggested distinct pathogenesis for the development of Nef-induced hematopoietic cell perturbations and kidney disease.

The present study was designed to identify the Nef-expressing cell subset involved in the development of kidney pathology. The results indicate that kidney disease in CD4C/HIV Tg mice arises independently of hematopoietic cells and is associated with the expression of HIV-1 Nef in kidney parenchymal cells, especially mesangial cells, and shares many features with human HIVAN. The disease is less severe when *Src* is deleted and much improved in the absence of *Hck/Lyn*.

Materials and Methods

Mice

CD4C/HIV-Nef, founder line F27367 (previously designated CD4C/HIV^{MutG} [28]; coding only for Nef), CD4C/HIV^{MutA}[28] [coding for regulator of expression of virion proteins (Rev), envelope (Env), and Nef], CD4C/HIV^{MutH} (coding for all *HIV-1* genes, except *nef*),[28] CD4C/HIV–green fluorescent protein (GFP)[40] (now designated CD4C/GFP), CD4C/reverse tetracyclin transactivator (rtTA) and tetracycline response element (TRE)/HIV-Nef[41] Tg mice, and gene-deficient (knockout) CD8,[42] μMT,[43] CD3ε,[44] J_H,[45] macrophage inflammatory protein-1α,[46] monocyte chemoattractant protein (MCP)-1,[47] CCR-2,[48] CCR-5,[49] CX3CR-1,[50] Bax,[51] p53,[52] tumor necrosis factor (TNF)-α,[53] tumor necrosis factor receptor 2 (TNF-R2),[54] TNF-related apoptosis inducing ligand (TRAIL; line 2041)[55] (Tactonic/Amgen, Seattle, WA), nitric oxide (NO) synthase 3 [endothelial NO synthase (eNOS)],[56] inducible NO synthase,[57] Fyn,[58] Hck,[59] Fgr,[59] Lck/Yes novel tyrosine kinase (Lyn),[60] Src,[61] and Lck[62] have been described previously. μMT, J_H, Bax, p53, TNF-α, TNF-R2, eNOS, Fyn, Src, and Lck knockout mice were from the Jackson Laboratory (Bar Harbor, ME). Liver/lymph node–specific intercellular adhesion molecule-3–grabbing non-integrin (L-SIGN)/GFP transgene was constructed by ligating the 753-bp GFP fragment followed by the SV40 polyadenylation site (900 bp) within exon 4 included in the 9.8-kbp NheI-SacI fragment of the human *L-SIGN* gene, comprising sequences upstream of exon 1, exons 1, 2, and 3, and part of exon 4 harboring a mutation of its ATG codon. CD4C/sd19 transgene was constructed by ligating the 500-bp *sd19* fragment into the MluI-NotI sites (nucleotides 8800 and 9420 of NL4-3) of CD4C/SHIV-*nef* DNA,[63] thus replacing the *nef* sequences.

Tg mice were generated by injecting DNA construct in 1-day–old embryos, as previously described.[27,28] At least three founders, expressing the transgene faithfully, were expanded for each strain. For most experiments, founders were bred with C3H/HeNHsd (Harlan, Indianapolis, IN) mice as heterozygous for more than six generations, before being studied. For experiments on some gene deficiency (Supplemental Table S1), mice were bred as above for more than six generations with C57BL/6 mice. For experiments on genetic susceptibility (Supplemental Table S2), mice were bred with the indicated mouse strains as heterozygous for more than six generations before being assessed, except for 129/J and DBA/2J Tg mice, which were bred for only four generations. Animals were kept in specific pathogen-free rooms.

Assessment of Kidney Histopathology

Kidney sections ($n = 4$ per mouse) were assessed, and lesions were scored semiquantitatively (scores 1 to 4), essentially as described before.[39] Extent of glomerulosclerosis and number of glomeruli affected, severity of tubular dilatation, number of microcysts, as well as extent of tubulo-interstitial infiltration were evaluated independently.

Culture of Glomeruli

Fresh glomeruli were purified with magnetic beads, as described previously,[64] and incubated with fibrolife medium (Lifeline Cell Technology, Frederick, MD; LM-0001 and LS-

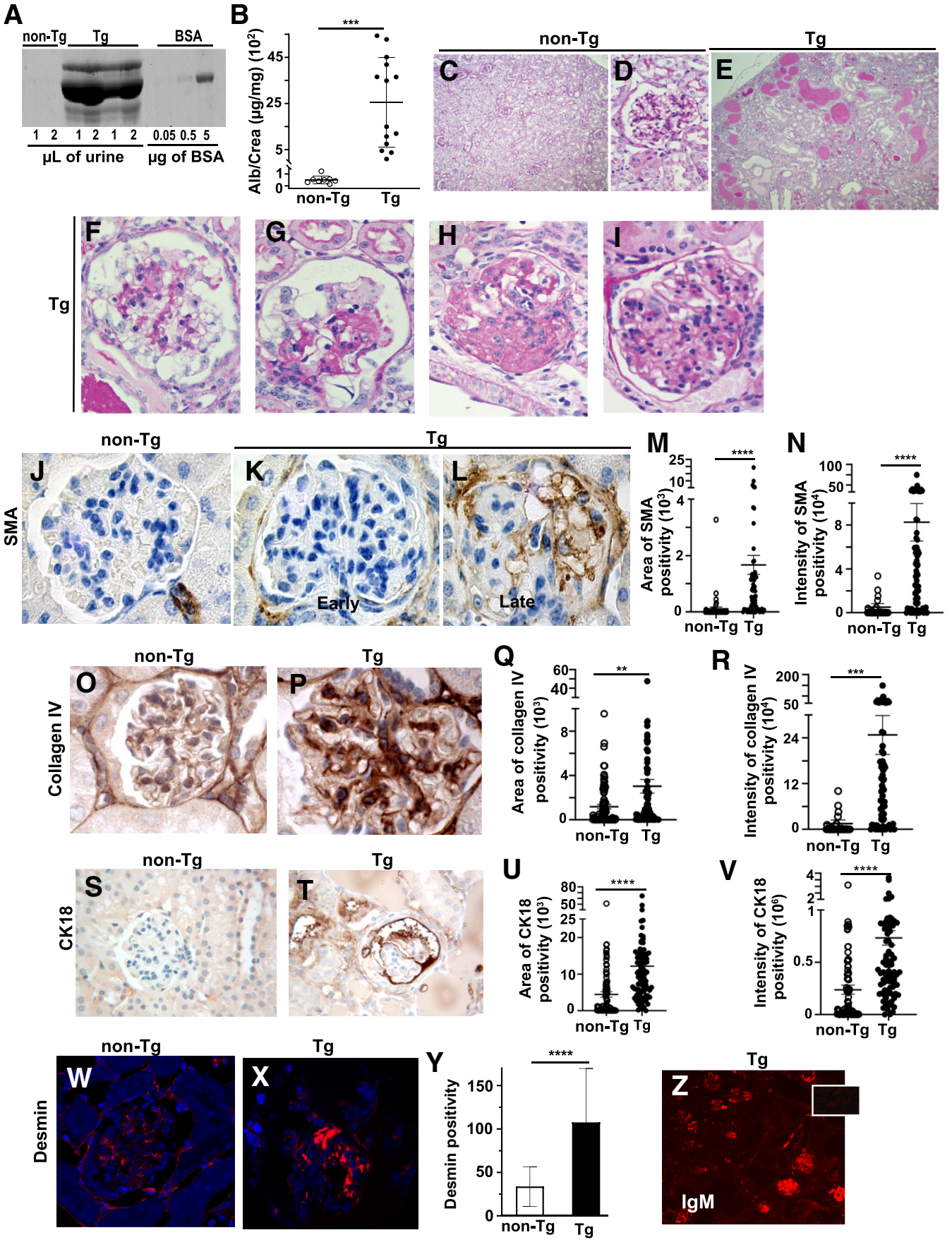
A
non-Tg
Tg
BSA
1 2 1 2 1 2
0.05 0.5 5
μL of urine
μg of BSA
B
***
Alb/Crea (μg/mg) (10²)
45
25
5
1
0
non-Tg
Tg
non-Tg
Tg
C
D
E
Tg
F
G
H
I
non-Tg
Tg
SMA
J
K
L
Early
Late
M
****
Area of SMA positivity (10³)
25
10
4
2
0
non-Tg
Tg
N
****
Intensity of SMA positivity (10⁴)
100
50
8
4
0
non-Tg
Tg
non-Tg
Tg
Collagen IV
O
P
Q
**
Area of collagen IV positivity (10³)
60
40
8
4
0
non-Tg
Tg
R
***
Intensity of collagen IV positivity (10⁴)
200
50
24
12
0
non-Tg
Tg
non-Tg
Tg
CK18
S
T
U
****
Area of CK18 positivity (10³)
80
50
25
20
10
0
non-Tg
Tg
V
****
Intensity of CK18 positivity (10⁶)
4
2
1
0.5
0
non-Tg
Tg
non-Tg
Tg
Desmin
W
X
Y
****
Desmin positivity
150
100
50
0
non-Tg
Tg
Tg
Z
IgM

1038) in fibronectin-coated (Sigma, St. Louis, MO; F0895) Petri dishes. For observation and image analysis, the culture dishes were not moved for a 24-hour period. For fluorescence-activated cell sorting (FACS) analysis, purified mouse glomeruli were further digested with collagenase (Sigma; C5138-1G) at 2.4 mg/mL and deoxyribonuclease (Sigma; DN-25) at 100 U/mL during 1.5 hours at 37°C (with frequent pipetting) in absence of trypsin found to interfere with CD31 labeling.

Tissue Preparation

Mice were sacrificed, and kidneys were perfused with phosphate-buffered saline 1× and 4% paraformaldehyde, fixed for 1 hour in 4% paraformaldehyde, incubated overnight in 10% sucrose, followed by 4 hours of incubation in 20% sucrose at 4°C, and then frozen in OCT medium and processed for immunofluorescence (IF), as previously described.[28,65] Otherwise, tissues were embedded in paraffin using a Shandon tissue infiltrator (hematoxylin and eosin), as described previously,[29,65] and processed for immunohistochemistry (IHC) or periodic acid—Schiff and periodic Schiff—methenamine staining.

Cell Proliferation

Mice were sacrificed by anesthesia with tribromoethanol (Avertin) 2 weeks following bromodeoxyuridine (BrdU; Sigma) administration (800 μg/mL drinking water) and perfused, using an intracardiac needle, first with phosphate-buffered saline and then with 4% paraformaldehyde, as described before.[35,65] BrdU-positive cells on tissue sections were detected with the BrdU *in situ* detection kit II (BD Biosciences, San Jose, CA). The technique was essentially that recommended by the manufacturer. Kidneys were embedded in paraffin blocks together with several other tissues, including small intestine and inguinal lymph nodes. These internal positive controls (intestinal epithelial cells in deep crypts and clusters of lymph node follicular cells were BrdU positive) were checked before analysis and used to exclude a false BrdU signal.

Antibodies

Antibodies (Abs) against WT-1 (Santa Cruz Biotechnology, Dallas, TX; SC-192), synaptopodin (Research Diagnostic Inc., Flanders, NJ; RDI-PRO65194), α8 integrin (R&D, Minneapolis, MN; AF4076), smooth muscle actin (SMA; Sigma; A2547), factor VIII (Dako, Santa Clara, CA; A0082), IgM (SouthernBiotech, Birmingham, AL; 1020-07), collagen IV (Abcam, Cambridge, UK; Ab 13,966), fibronectin (Miles Laboratories, Pittsburgh, PA), desmin (Dako; M0760), cleaved caspase-3 (Biocare Medical, Pacheco, CA; CP229B), cytokeratin (CK)18 (Santa Cruz Biotechnology; SC-28264), CD31-biotin, platelet endothelial cell adhesion molecule (BD Biosciences), CD44 (IM7; BD Biosciences), or Src-suppressed protein kinase C substrate (Thermo Fisher Scientific, Waltham, MA; PA1-29372) were purchased from the indicated suppliers. For IHC, horseradish peroxidase—conjugated secondary Abs were used. For IF, fluorochrome-conjugated secondary Abs used included the following: anti—sheep-Alexa 488, anti—rabbit-Alexa 633, and anti—mouse-Alexa 555 (all from Molecular Probe, Eugene, OR) or biotin (BD Biosciences), anti—mouse-Alexa 594 (R&D) anti—rabbit-Alexa 594, anti—goat-Alexa 555, and anti—rat-Alexa 568 (Invitrogen, Waltham, MA; and R&D). With biotin-conjugated Abs, streptavidin conjugated to Alexa 546 or to Texas Red (Molecular Probe) was used. Alternatively, for some IF experiments, some antibodies were directly conjugated. For flow cytometry of mouse immune cells, phycoerythrin (PE)-, PE-cyanine 7 (PECy7)-, allophycocyanin (APC)-, or fluorescein isothiocyanate—conjugated antibodies against mouse CD4, CD8α, CD11b, CD11c, and B220 as well as their isotypic controls (rat IgG2a, rat IgG2b, and Armenian hamster IgG1) were purchased from Cedarlane (Burlington, ON, Canada) or BD Biosciences.

Mouse glomerular cells were analyzed by FACS with anti-CD45.2, anti—peridinin chlorophyll protein complex (PERCP)-Cy5.5, anti—CD31-biotin (BD Pharmigen,

Figure 1 Renal pathology of CD4C/HIV-Nef transgenic (Tg) mice represents a collapsing focal segmental glomerulosclerosis (FSGS). **A** and **B:** Evaluation of albuminuria in non-Tg and Tg mice. Urine was run on SDS-PAGE along with control bovine serum albumin (BSA) at different concentrations (**A**), and ratios of albumin (Alb)/creatinine (Crea) concentration were measured (**B**). **C**—**I:** Representative kidney sections stained with periodic acid—Schiff. **E:** Tubular dilatations forming microcysts, with interstitial fibrosis and monocytic infiltration observed in Tg mice. **F** and **G:** FSGS is seen in glomeruli of Tg mice, some presenting with collapsing features, including segmental to global collapse of the tuft and hypertrophic, hyperplasic vacuolated podocytes. **H:** Other FSGS lesions presented with segmental solidification of the tuft by matrix material, hyaline deposits, and adhesion. **I:** Mild mesangial cell hypercellularity in less affected Tg glomeruli. **J**—**L**, **O**, **P**, **S**, and **T:** Immunohistochemistry on kidney sections with antibodies against smooth muscle actin (SMA; **J**—**L**), collagen IV (**O** and **P**) and cytokeratin 18 (CK18; **S** and **T**). **M**, **N**, **Q**, **R**, **U**, and **V:** Glomerular area (**M, Q**, and **U**) and intensity (**N, R**, and **V**) of immunoreactivity were quantitated on 18 to 25 randomly chosen glomeruli per mouse on groups of three to five non-Tg and four to five Tg mice. Relative values (pixels) for each glomerulus are shown as a dot and were pooled. **K** and **L:** SMA staining is increased in Tg mice in late (**L**), but not in early (**K**), stages. **K**, **L**, and **T:** Strong labeling of periglomerular and parietal Tg cells with anti-SMA (**K** and **L**) and anti-CK18 (**T**) antibody (Ab). **W** and **X:** Confocal immunofluorescence with Ab against desmin. **Y:** Quantification of glomerular desmin staining (mean of voxels count) was performed on 60 randomly chosen glomeruli. **Z:** Detection of IgM in glomeruli of Tg mice by immunofluorescence microscopy with anti-mouse IgM monoclonal Ab. **Inset:** Portion of non-Tg kidney reacted with the same anti-IgM Ab. Statistical analyses were performed with the nested analysis of variance test with Bonferroni correction. For all these markers, staining in Tg glomeruli was variable, as documented in the dispersed values of area and intensity of immunoreactive positivity. $n = 40$ Tg mice (**E**). $^{**}P < 0.01$, $^{***}P < 0.001$, and $^{****}P < 0.0001$. Original magnification: ×100 (**C**, **E**, and **J**—**P**); ×400 (**D**, **H**, and **I**); ×600 (**F** and **G**); ×40 (**S**, **T**, **W**, and **X**); ×10 (**Z**).

Franklin Lakes, NJ), and anti-α8 integrin-biotin (R&D; BAF4076) as well as their respective isotype control (rat IgG 2b-biotin and goat IgG biotin) and streptavidin-APC conjugated.

IHC and IF

IHC was performed essentially as described.[29,65] After dewaxing of paraffin slides and rehydration, sections were treated with 0.3% hydrogen peroxide in phosphate-buffered saline, then blocked with 3% goat serum in phosphate-buffered saline for 30 minutes at room temperature before incubation with various Abs and their isotype control Abs for 1 hour at room temperature, except for WT-1 at 37°C. This was followed by incubation with horseradish peroxidase–conjugated secondary Abs. Finally, the positive signal was visualized with 4.4-diaminobenzidine tetrahydrochloride. For IF, frozen sections were fixed for 10 minutes at room temperature in 10% formalin, permeabilized with 0.5% Triton X-100 for 10 minutes at room temperature, and blocked with 10% fetal bovine serum inactivated, 2% bovine serum albumin, and 0.3% Triton X-100 for 1 hour at room temperature. Incubation with primary Ab overnight at 4°C was followed by incubation with fluorochrome-conjugated secondary Ab for 40 to 60 minutes at room temperature, as previously described.[40] Thicker (50 μm) sections were first permeabilized with 1% Triton for 30 minutes at room temperature and stained with Ab in suspension for approximately 12 hours at 4°C. Sections were mounted with Vectashield mounting medium with DAPI (Vector Laboratories, Inc., Newark, CA; number H-1200). Staining with most markers was in general more variable in Tg than in non-Tg glomeruli, most likely reflecting the focal nature of the disease.

Electron Microscopy

Mice were perfused with 2% glutaraldehyde in 0.1 mol/L, pH 7.4. cacodylate buffer (10 minutes). The perfused kidneys were further fixed in cacodylate buffer (2 hours) and therein rinsed with 20% sucrose. The fixed kidney tissues were cut into 1-mm blocks and subsequently prepared for electron microscopy.

Image Analysis

Quantification of kidney characteristics was performed on digital images of the relevant materials (hematoxylin and eosin–stained sections, GFP- or BrdU-positive and IHC horseradish peroxidase–positive sections of kidneys, and glomeruli in culture), by using Northern Eclipse 6.0 software (Empix Imaging, Mississauga, ON, Canada), essentially as described,[65] and Matlab Release 2020 b software (MathWorks Inc., Natick, MA). For all experiments assessing glomeruli, 15 to 25 randomly chosen glomeruli for each mouse were analyzed. The culture dishes or sections were scanned, and color images were captured by using Zeiss Axiophot supported with Northern Eclipse (Zeiss, Munich, Germany).

For cells growing out of glomeruli in culture, images in phase contrast of randomly chosen fields ($n = 10$ to 20) at ×10 or ×20, including at least one glomerulus, were taken. When necessary, images in fluorescence of the same field were also taken using the same conditions.

For quantitation of proliferation, randomly chosen images ($n = 15$ to 20) of BrdU-labeled sections were obtained at ×40. BrdU-positive cells, total glomerular cells, and total parietal epithelial cells were counted separately, except when glomerular and parietal cells adhered to one another.

For quantitation of WT-1 staining, images of kidney sections ($n = 30$ to 50) were taken randomly from animals showing mild and severe kidney disease, as determined by hematoxylin and eosin staining. The number of WT-1–positive cells per glomerulus was counted. The *t*-test was employed to compare Tg and non-Tg groups.

Immunofluorescence staining of kidney sections (10 to 20 μm thick) and of purified kidney glomerular cells for α8 integrin, synaptopodin, CD31, SMA, desmin, and renin (×40 oil) was analyzed by confocal microscopy using Zeiss LSM 700, LSM 710, and Zen software (version 2011 for LSM 700 and version 2009 for LSM 710). Analysis and quantification of GFP expression with or without additional staining was performed with Volocity software version 6 (Quorum Technologies, Puslinch, ON, Canada) and Imaris ×64 three-dimensional (for 50-μm–thick section) software version 8.2.1 (Oxford Instruments, Zürich, Switzerland). The GFP levels represent summation of intensity values of green (GFP) intersecting with red (cell-specific markers) on stained cells (colocalization). Percentage of GFP-positive cells and percentage of CD31-, synaptopodin-, or α8 integrin-positive cells expressing GFP were obtained by analysis of a total of 780 to 1950 cells.

FACS Analysis

Flow cytometry was performed as previously published.[35] Acquisition was performed on FACSCalibur (BD Biosciences), BD-LSR (BD Biosciences), or Cyan (Beckman Coulter Canada, Mississauga, ON, Canada). Data were analyzed using the CellQuest Pro software version 6.0 (BD Biosciences) or FlowJo software version 9.9.5 (BD Biosciences). Cell sorting was performed on a Mo-Flo cell sorter (Cytomation, Inc., Fort Collins, CO).

Western Blot Analysis

Protein expression was assessed by Western blot analysis of lymphoid organs or purified glomeruli from different founders using rabbit anti-Nef antisera, as described previously.[28] Proteins were visualized by incubating the membranes with secondary antibodies coupled to Alexa 680

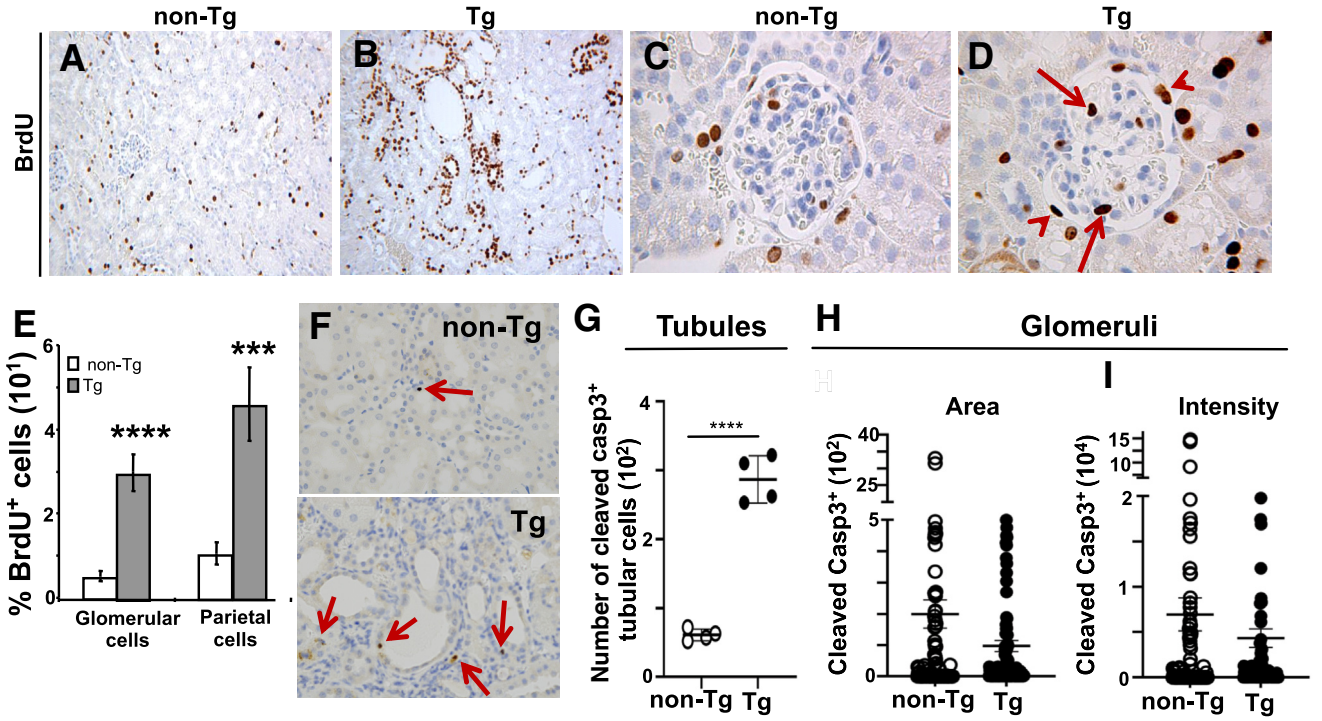

Figure 2 Renal pathology of CD4C/HIV-Nef transgenic (Tg) mice is associated with enhanced kidney cell proliferation and enhanced tubular, but minimal glomerular, apoptosis. **A**—**D:** Proliferation was assessed after bromodeoxyuridine (BrdU) incorporation *in vivo*, in non-Tg (**A** and **C**) and Tg (**B** and **D**) mice. Incorporated BrdU was detected by immunohistochemistry (IHC). **A**—**D:** Images at low (**A** and **B**) or high (**C** and **D**) magnification. **B** and **D:** Incorporated BrdU was greatly enhanced in Tg tubular (**B**), glomerular (**arrows**; **D**), and parietal (**arrowheads**; **D**) epithelial cells. **E:** Quantitative analysis. The percentage of BrdU-positive cells was calculated from the total number of glomerular or parietal cells and analyzed by the *t*-test. A total of 23 non-Tg and 18 Tg glomeruli per mouse from two non-Tg and three Tg mice were counted. **F**—**I:** Apoptosis was assessed by IHC with anti—cleaved caspase-3 (casp3) antibody. **F:** Representative images of non-Tg (**top panel**) and Tg (**bottom panel**) kidneys showing cleaved casp3-positive cells (**red arrows**). **G:** Quantification of the number of cleaved casp3-positive tubular cells counted in all ×40 fields of one kidney per mouse, excluding glomeruli, in four non-Tg and four Tg mice. Data were analyzed by *t*-test. **H** and **I:** Quantification of cleaved casp3 staining in glomeruli was performed on 18 to 25 randomly chosen glomeruli per mouse on groups of six non-Tg and five Tg mice, as in Figure 1, M and N. **H** and **I:** Relative area (**H**) and intensity (**I**) of glomerular immunoreactive materials (pixels) are shown for each group and analyzed by nested analysis of variance. ***$P < 0.001$, ****$P < 0.0001$. Original magnification: ×10 (**A** and **B**); ×40 (**C** and **D**); ×20 (**F**).

fluorochrome, followed by scanning with Odyssey infrared imaging system (LI-COR, Lincoln, NE).

Measurement of Albumin and Creatinine

Urine albumin was visualized by PAGE. Quantitation was also performed by enzyme-linked immunosorbent assay (Bethyl Laboratories Inc., Montgomery, TX). Urine creatinine (number 32263991 to 190) was measured with kits from Cobas Integra (Roche Diagnostics, Indianapolis, IN).

Statistical Analysis

Statistical analysis was performed in most cases using the unpaired two-tailed *t*-test. In case of comparison of ratios, a one-sample *t*-test was used. One- or two-way analysis of variance with Bonferroni correction, where appropriate, was used for comparison of multiple samples. Nested analysis of variance with Bonferroni correction was used for comparison of pooled glomerular values.

Results

HIVAN in CD4C/HIV-Nef Tg Mice

The renal disease of CD4C/HIV Tg mice leads to increased serum creatinine and urea[66] and albuminuria (Figure 1, A and B). Pathologic evaluation with hematoxylin and eosin or periodic acid—Schiff (Figure 1, C—I) was performed. Light microscopy examination of Tg kidneys revealed severely affected glomeruli by global and focal segmental glomerulosclerosis (Figure 1E). Some of the segmental lesions demonstrated the characteristic features of collapsing glomerulopathy, including segmental collapse of the glomerular tuft with hypertrophy and hyperplasia of the overlying visceral epithelial region, showing enlarged and vesicular nuclei with prominent nucleoli (Figure 1, F and G). The cytoplasm of visceral epithelial cells was often vacuolated, and resorption droplets were occasionally seen. Other segmental glomerular lesions demonstrated solidification of the tuft by matrix material, hyalinoses, and adhesion to the Bowman capsule (Figure 1H). Staining for SMA (Figure 1,

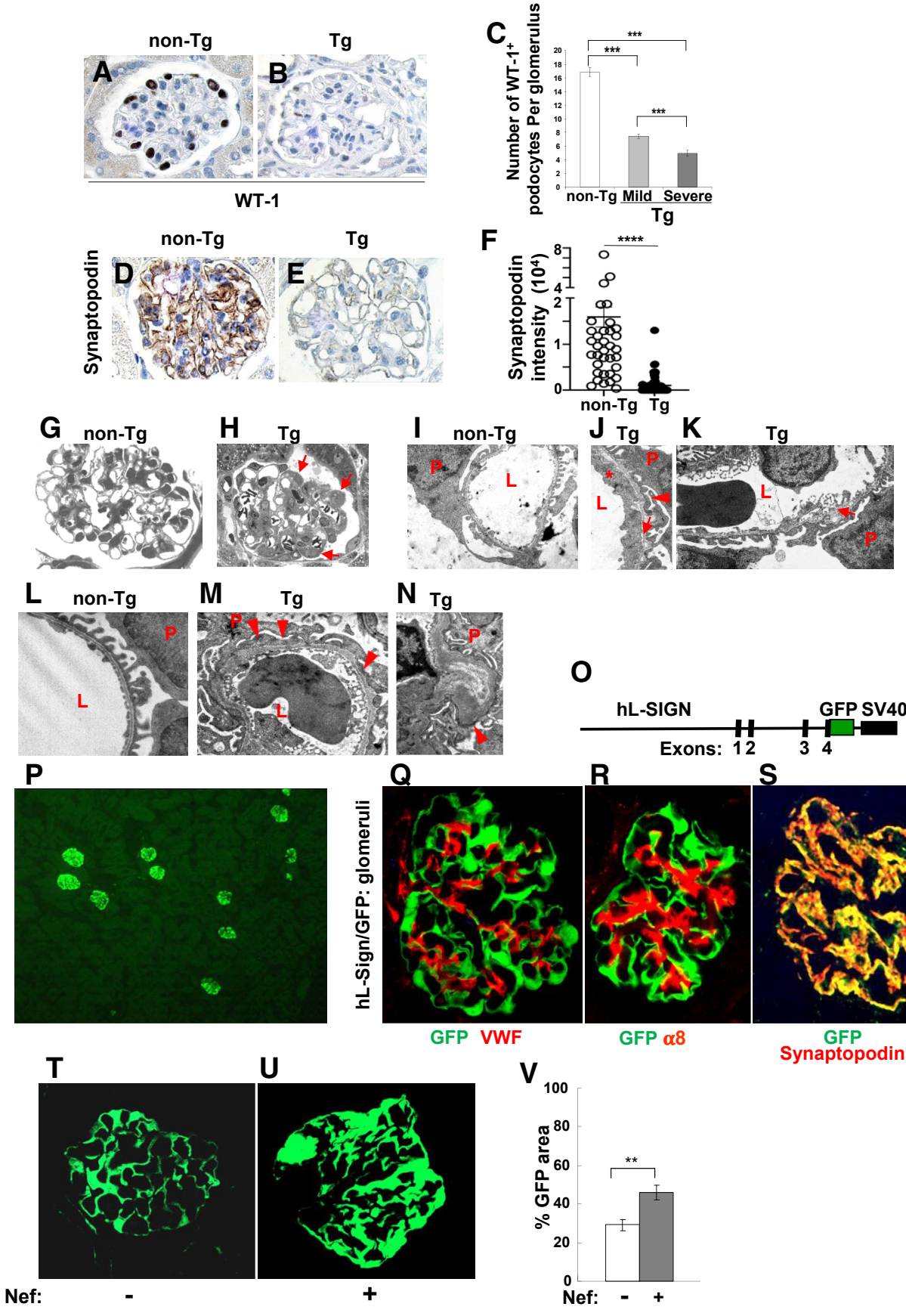
non-Tg
Tg
A
B
WT-1
C
Number of WT-1+ podocytes Per glomerulus
***
***
***
non-Tg Mild Severe
Tg
non-Tg
Tg
Synaptopodin
D
E
F
Synaptopodin intensity (10⁴)
****
non-Tg Tg
G non-Tg
H Tg
I non-Tg
J Tg
K Tg
P
L
L non-Tg
M Tg
N Tg
O
hL-SIGN
GFP SV40
Exons: 1 2 3 4
P
Q
R
S
hL-Sign/GFP: glomeruli
GFP VWF
GFP α8
GFP Synaptopodin
T
U
Nef: - +
V
% GFP area
**
Nef: - +

J−N), collagen IV (Figure 1, O−R), CK18 (Figure 1, S−V), desmin (Figure 1, W−Y), and fibronectin (Supplemental Figure S1) was greatly enhanced in Tg glomeruli. Interestingly, at early stages of the disease, SMA (Figure 1K) and desmin (Figure 1X) positivity was largely confined to cells around the glomeruli, some of them with the appearance of parietal cells. Staining with CK18, a parietal cell marker, also showed enhanced positivity of Tg glomerular, including parietal cells (Figure 1T), the latter possibly activated (see below), because this marker is known to be up-regulated in activated parietal cells.[67] In addition, deposition of IgM was present in glomeruli of Tg mice (Figure 1Z), consistent with the detection of similar IgM aggregates on hearts of the same CD4C/HIV Tg mice.[29] Tubulo-interstitial alterations included tubular atrophy, interstitial fibrosis, and interstitial accumulation of mononuclear cells mostly composed of lymphocytes. Numerous tubular dilatations containing proteinaceous material were seen, resulting in tubular microcysts (Figure 1E). Intratubular leukocytes were occasionally present. Tubular epithelial cells showed acute tubular injury, characterized by simplification and loss of brush border, as well as regenerative changes.

Human HIVAN is accompanied by significant proliferation of glomerular cells.[6] Proliferation of kidney cells of CD4C/Nef Tg mice was further assessed by detection of BrdU incorporated into DNA, using IHC. It showed a significantly enhanced proliferation of Tg tubular (Figure 2, A and B), parietal (Figure 2, C−E), and glomerular (Figure 2, C−E) cells relative to non-Tg ones. A large proportion (approximately 55%) of BrdU-positive glomerular cells (115 counted) are desmin positive, as assessed by colocalization, strongly suggesting that some of the desmin-positive cells initially found in parietal area may represent proliferating parietal cells.

Because proliferation is often accompanied by enhanced apoptosis, the extent of apoptosis in Tg kidneys was performed by using IHC with anti−cleaved caspase-3 Abs (Figure 2, F−I). These analyses showed an enhanced number of apoptotic tubular cells in Tg mice relative to non-Tg mice (Figure 2, F and G). However, Tg glomeruli did not show an increased number of apoptotic cells relative to non-Tg ones (Figure 2, H and I). Deletion of a few genes involved in apoptosis (*Fas*, *Fasl*, *Casp1*, and *Tnfrsf1a*) was previously shown to not have an impact on the development of kidney disease in Tg mice.[68] Deletion of additional genes involved in apoptosis (*Trp53*, *Tnfsf10*, *Tnf*, *Tnfrsf1b*, and *Bax*), and some of which implicated in the pathogenesis of FSGS (*Tnf* and *Bax*), was investigated.[69−72] Deleting these genes had no detectable effect on kidney disease (Supplemental Table S1).

Ultrastructural studies showed extensive to diffuse foot process effacement, with irregular thickening and segmental splitting of the basement membrane in Tg glomeruli (Figure 3, K and M), relative to non-Tg ones (Figure 3, I and L). Endothelial cells often exhibited loss of fenestrations (Figure 3K). Thus, it appears that many, but not all, features of the kidney disease of CD4C/HIV Tg mice are typical of other FSGS developing in mice.

Podocytes of CD4C/HIV-Nef Tg Mice Show Signs of Dedifferentiation, Hypertrophy, and Minimal Proliferation

Because glomerulosclerosis is mostly a disease of podocytes, this cell subset was evaluated first. The intensity of staining of podocytes for WT-1 (Figure 3, A−C) or synaptopodin (Figure 3, D−F) was highly reduced in most (90%) Tg glomeruli relative to controls, probably reflecting loss of podocytes and their dedifferentiation, similar to that documented in human HIVAN.[6] Electron microscopy revealed hypertrophy of Tg podocytes (Figure 3H) relative to non-Tg ones (Figure 3G). Foot process effacement in Tg podocytes was already apparent at 16 days of age (Figure 3, J and K) and advanced at 40 days (Figure 3, M and N). Focal thickening and wrinkling of glomerular basement membrane was already visible at early stage (Figure 3, J and K), and diffuse thickening and folding was present at later stage (Figure 3, M and N).

To further study the fate of podocytes, human (h)L-SIGN/GFP reporter Tg mice (Figure 3O) expressing *Gfp* in kidney glomeruli (Figure 3P), specifically in podocytes (Figure 3,

Figure 3 Podocyte dedifferentiation and foot process effacement in CD4C/HIV-Nef transgenic (Tg) mice. **A**−**F:** Representative immunohistochemical images of kidney sections with antibodies against WT-1 (**A**−**C**) or synaptopodin (**D**−**F**). **B** and **C**: Decreased WT-1 staining in Tg glomeruli, representative of 90% of Tg glomeruli. Some Tg glomeruli (5% to 10%) stain as non-Tg ones. **F:** Quantification of synaptopodin staining in glomeruli performed on 18 to 25 randomly chosen glomeruli per mouse on groups of three non-Tg and three Tg mice, as in Figure 1, M and N. Relative intensity (pixels) for each glomerulus is shown as an open (non-Tg) or closed (Tg) dot and was pooled. **G**−**N:** Electron microscopy. **G**−**N:** Young (16-day−old; **I**−**K**) or older [40-day−old (**G**, **H**, **L**, and **M**) or 54-day−old (**N**)] non-Tg and Tg mice were used. **G** and **H:** Podocyte hypertrophy (**arrows**) observed in Tg (**H**), but not in non-Tg (**G**), mice. **J**, **K**, **M**, and **N:** Foot process effacement (**arrowheads**), endothelial cell swelling (**asterisk**), and focal splitting of glomerular basement membrane (GBM; **arrows**) seen in 16-day−old Tg mice (**J** and **K**) and advanced in 40-day−old Tg mice (**M** and **N**). **M** and **N:** Diffuse thickening and folding of GBM. **O**−**S:** Expression of green fluorescent protein (GFP) in podocytes of human liver/lymph node−specific intercellular adhesion molecule-3−grabbing non-integrin (hL-SIGN)/GFP reporter mice. **O:** Structure of the hL-SIGN/GFP transgene. **P:** Low magnification showing GFP expression in glomeruli. This glomerular pattern of GFP expression was observed in four independent Tg founder lines. **Q**−**S:** Confocal microscopy with antibody against von Willebrand factor (VWF; **Q**), α8 integrin (**R**), and synaptopodin (**S**). Colocalization was observed only with synaptopodin labeling, indicating that the GFP-positive cells represent podocytes. **T**−**V:** Early hypertrophy of podocytes in Nef-expressing Tg mice. Kidney sections were prepared from (hL-SIGN/GFP × CD4C/HIV-Nef) double and single hL-SIGN/GFP Tg mice, and areas occupied by GFP were measured. **T**−**V:** Representative image of glomeruli in young mice (**T** and **U**) and quantification of glomeruli GFP areas (**V**). $n = 4$ non-Tg and 4 Tg mice (**G**−**N**); $n = 2$ (hL-SIGN/GFP × CD4C/HIV-Nef) double Tg mice and single hL-SIGN/GFP Tg mice (**T**−**V**). $^{**}P < 0.01$, $^{***}P < 0.001$, and $^{****}P < 0.0001$. Original magnification: ×100 (**A**, **B**, **D**, **E**, **G**, **H**, and **Q**−**U**); ×7500 (**I**−**K**); ×15,000 (**L**−**N**); ×10 (**P**). L, capillary lumen; P, podocyte.

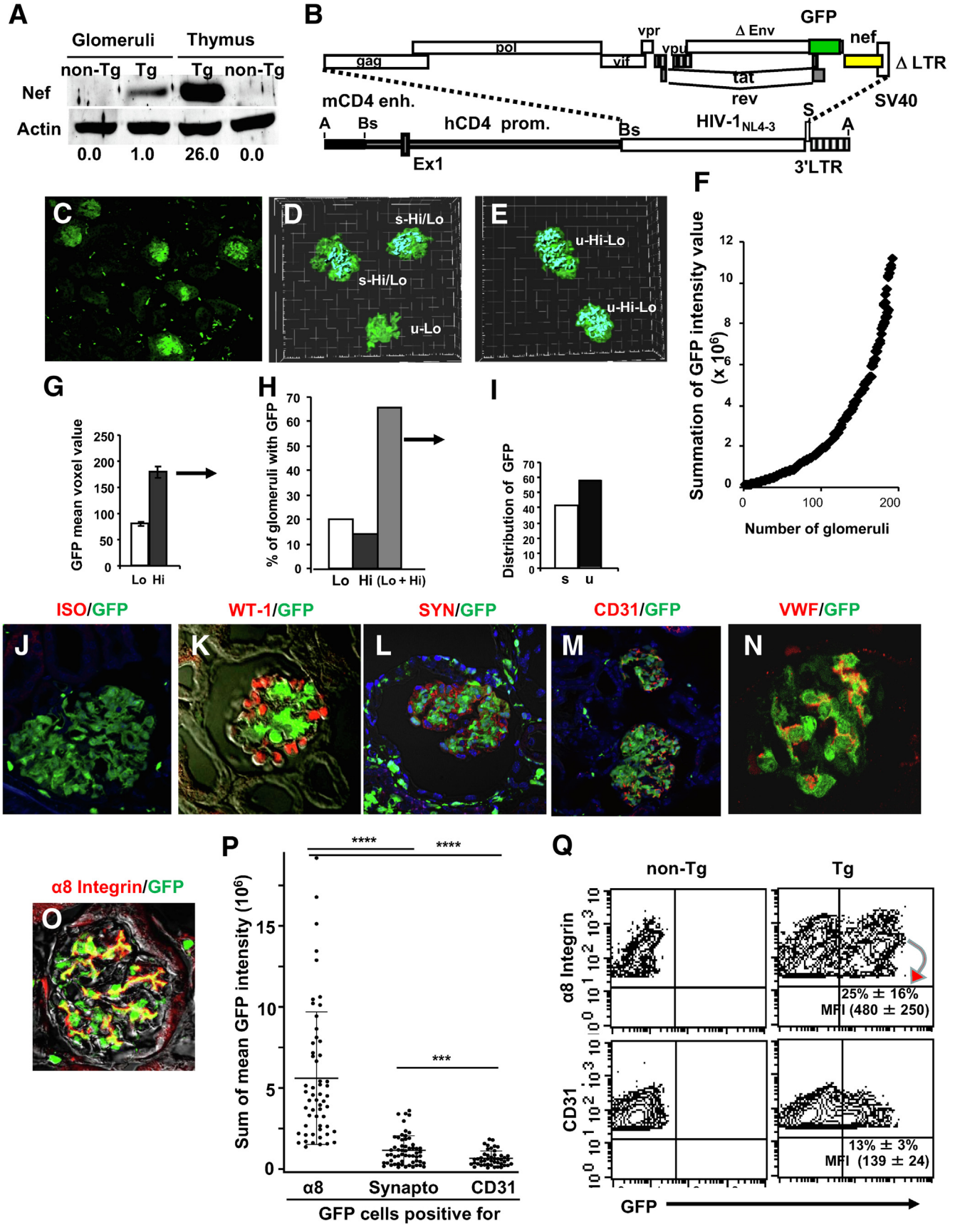
A
Glomeruli
Thymus
non-Tg
Tg
Tg
non-Tg
Nef
Actin
0.0
1.0
26.0
0.0
B
GFP
vpr
Δ Env
nef
pol
vpu
gag
vif
Δ LTR
tat
rev
mCD4 enh.
SV40
A
Bs
hCD4 prom.
Bs
HIV-1NL4-3
S
A
Ex1
3'LTR
C
D
s-Hi/Lo
s-Hi/Lo
u-Lo
E
u-Hi-Lo
u-Hi-Lo
F
Summation of GFP intensity value (x 10^6)
Number of glomeruli
G
GFP mean voxel value
Lo
Hi
H
% of glomeruli with GFP
Lo
Hi (Lo + Hi)
I
Distribution of GFP
s
u
ISO/GFP
WT-1/GFP
SYN/GFP
CD31/GFP
VWF/GFP
J
K
L
M
N
α8 Integrin/GFP
O
P
Sum of mean GFP intensity (10^6)
****
****
***
α8
Synapto
CD31
GFP cells positive for
Q
non-Tg
Tg
α8 Integrin
CD31
25% ± 16%
MFI (480 ± 250)
13% ± 3%
MFI (139 ± 24)
GFP

Q–S), were used. Analysis of GFP-tagged podocytes in double (hL-SIGN/GFP × CD4C/Nef) Tg mice showed hypertrophy of GFP-expressing podocytes (enhanced GFP-positive surface area in diseased glomeruli) (Figure 3, T–V), with minimal proliferation, as assessed by BrdU labeling. Among the BrdU-positive glomerular cells (195 counted) in Nef-expressing mice, only a small fraction (approximately 3%) represented GFP-positive podocytes, as assessed by colocalization using confocal microscopy. Together, these results indicate that the modest podocyte proliferation observed (Figures 1I and 3H) is unlikely to account for the more important glomerular cell proliferation detected in Tg mice (Figure 2E).

HIV-1 Nef Protein Is Sufficient to Induce HIVAN in Tg Mice

CD4C/Nef Tg mice (encoding only *nef* among the known genes of HIV-1, with all the other genes being inactivated) develop kidney disease, whereas CD4C/HIV-ΔNef Tg mice (encoding all HIV genes, except *nef*) do not.[28] These experiments indicate that the *nef* gene is likely involved in the development of kidney disease, but do not show that Nef protein was involved. Other yet undiscovered *HIV-1* gene(s) or genetic product(s) could be encoded by the *nef* sequences and participate, along with Nef, in the development of kidney disease. To rule this possibility out, an anti-Nef llama nanobody was used which was able to block all known functions of Nef protein *in vitro* and *in vivo*, including in T cells of CD4C/Nef Tg mice.[73] Tg mice (CD4C/sd19) expressing the *sd19* anti-Nef nanobody under the regulation of the same CD4C promoter used in CD4C/Nef Tg mice (Supplemental Figure S2A) were generated. As expected from previous work with hematopoietic cells transduced with retroviral vector encoding this anti-Nef nanobody,[73] the percentage of $CD4^+$ T cells from double (CD4C/Nef × CD4C/sd19) Tg mice was increased, and a large proportion of them did not exhibit Nef-induced CD4 down-regulation (Supplemental Figure S2B). In addition, these double Tg mice showed lower albuminuria (Supplemental Figure S2C) and less severe pathologic kidney lesions (Supplemental Figure S2D) than single CD4C/HIV-Nef Tg mice, strongly suggesting that Nef protein itself is involved in the development of HIVAN in Tg mice.

Hematopoietic Cells Do Not Contribute to the Development of HIVAN in CD4C/HIV Tg Mice

Kidney disease of CD4C/HIV Tg mice can not be transferred by transplantation of Tg hematopoietic cells[34] and develops in absence of $CD4^+$ T cells.[35] Herein, kidney disease was not abrogated in homozygous (−/−) C57BL/6 CD4C/Nef or C3H CD4C/HIV^{MutA} Tg mice bred on *Cd8*, *Ighm*, *Cd3e*, *Cd3e/Igh-J*, or *Cd3e/Ighm* gene-deficient background and was undistinguishable from disease in heterozygous (+/−) Tg mice (Supplemental Table S1), indicating that T and B cells are not required for its development. Levels of normal T cell expressing and secreting (RANTES) and MCP-1 chemokines, involved in macrophage recruitment, are elevated in CD4C/HIV Tg mice.[27,66] This prompted the investigation of the contribution of chemokine pathways to the development of kidney disease. CCR-2 and MCP-1 have been implicated in FSGS glomerular injury.[74,75] Tg mice, bred on background homozygous (−/−) deficient for macrophage inflammatory protein 1α (*Ccl3*), *Ccl2*, *Ccr2*, *Cx3cr1*, or *Ccr5* gene still developed severe kidney disease (Supplemental Table S1). These results are consistent with the absence of kidney disease in Tg mice expressing Nef in macrophages (human CD68/HIV-Nef) or dendritic cells (CD11c/HIV-Nef).[34]

Together, these results indicate that T and B cells as well as Nef-expressing macrophages and dendritic cells are not required for the development of kidney disease in CD4C/HIV Tg mice. Rather, HIVAN appears to be induced by Nef-expressing cells other than transplantable hematopoietic cells.

Nef Is Preferentially Expressed in Mesangial Cells and Often Focally Distributed in Glomeruli of CD4C/Nef Tg Mice

To identify which Nef-expressing cell subset was involved in the development of kidney disease in these Tg mice, parenchymal kidney cells were studied next. *In situ*

Figure 4 The regulatory sequences of the human *CD4* gene drive expression of green fluorescent protein (GFP) primarily in glomerular mesangial cells of transgenic (Tg) mice. **A:** Western blot analysis of protein extracts (100 μg) from purified glomeruli or thymus of non-Tg and CD4C/HIV-Nef Tg mice. **B:** Structure of the CD4C/GFP transgene. **C–E:** Fluorescent (**C**) or confocal (**D** and **E**) microscopy in kidney glomeruli of CD4C/GFP Tg mice to detect GFP expression. **D** and **E:** Representative images showing segmental (s) or uniform (u) distribution of GFP^{Hi} (Hi) and GFP^{Low} (Lo) cells. **F–I:** Quantification was performed with Volocity version 6 (**F**) or Imaris version 8.2.1 (**G–I**) software, comparing GFP expression between (**F**) or within (**G–I**) glomeruli, and recording levels of GFP expressing [low (Lo)] or [high (Hi)] mean voxels value (**G**), percentage of glomeruli with low or high GFP levels (**H**), as well uniform (u) or segmental (s) distribution (**I**) of GFP expression. Note nonuniform levels of expression. **J–O:** Confocal immunofluorescence with isotype control (ISO) antibody (Ab; **J**) or with Ab against WT-1 (**K**), synaptopodin (SYN; **L**), CD31 (**M**), von Willebrand factor (VWF; **N**), and α8 integrin (**O**) (all in red). **P:** Quantification of GFP intensity signal in GFP-positive cells stained for α8 integrin, synaptopodin (Synapto), or CD31. GFP/marker colocalization was analyzed on kidney tissue sections on 60 to 70 glomeruli by confocal microscopy and quantitated with Volocity software. Data are expressed as summation of intensity values (pixels). **Q:** Fluorescence-activated cell sorting profile of CD45.2-negative, GFP-positive glomerular cells of CD4C/GFP Tg mice labeled with the indicated antibodies or their isotype controls. Note the higher percentage of GFP^{Hi} cells labeled with anti-α8 integrin Ab. Also note that most CD31-positive cells are GFP^{Lo}. Number and percentage of α8 $integrin^+$ or $CD31^+$ cells in quadrant are given. Data from four experiments with 10 mice. $n = 200$ glomeruli (**F**); $n = 60$ glomeruli (**G–I**); $n = 10$ CD4C/GFP Tg mice (**Q**). $^{***}P < 0.001$, $^{****}P < 0.0001$. Original magnification: ×10 (**C**); ×20 (**D** and **E**); ×40 (**J–O**). A, AatII; Bs, BssHII; Ex1, exon 1; hCD4 promo, promoter of the human *CD4* gene; LTR, long terminal repeat; mCD4 enh., mouse CD4 enhancer; MFI, mean fluorescence intensity; S, SalI.

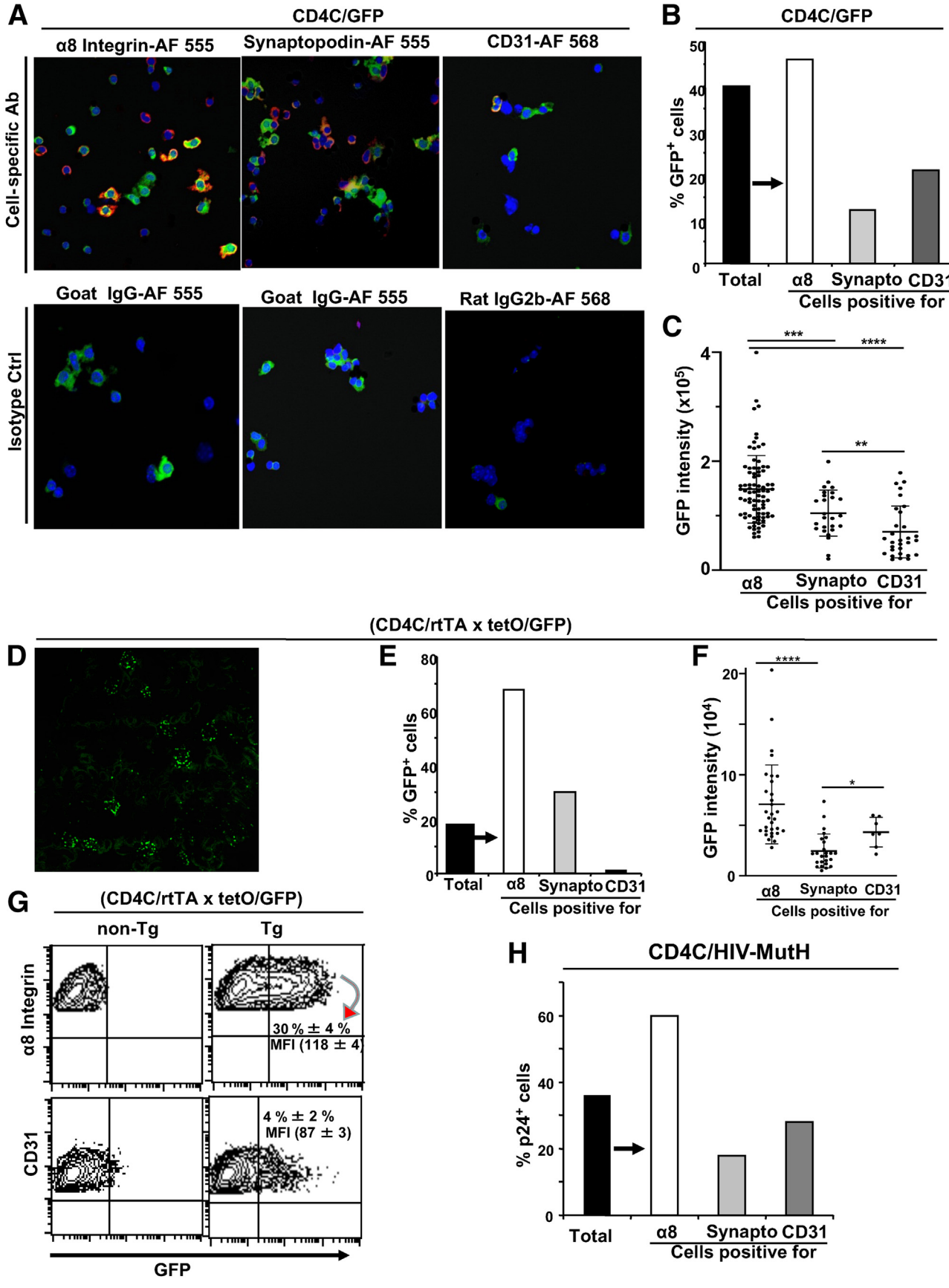
A
CD4C/GFP
α8 Integrin-AF 555
Synaptopodin-AF 555
CD31-AF 568
Cell-specific Ab
Goat IgG-AF 555
Goat IgG-AF 555
Rat IgG2b-AF 568
Isotype Ctrl
B
CD4C/GFP
% GFP+ cells
Total
α8
Synapto
CD31
Cells positive for
C
GFP intensity (x10^5)
***
****
**
α8
Synapto
CD31
Cells positive for
(CD4C/rtTA x tetO/GFP)
D
E
% GFP+ cells
Total
α8
Synapto
CD31
Cells positive for
F
GFP intensity (10^4)
****
*
α8
Synapto
CD31
Cells positive for
G
(CD4C/rtTA x tetO/GFP)
non-Tg
Tg
α8 Integrin
CD31
30 % ± 4 %
MFI (118 ± 4)
4 % ± 2 %
MFI (87 ± 3)
GFP
H
CD4C/HIV-MutH
% p24+ cells
Total
α8
Synapto
CD31
Cells positive for

hybridization has been used to detect HIV expression in glomeruli of CD4C/HIV Tg mice.[27] These findings were confirmed by the expression of Nef protein observed in total protein extracts from purified glomeruli by Western blot analysis (Figure 4A).

Because these two detection techniques do not allow the identification of glomerular cells permissive for CD4C-driven expression, a reporter Tg mouse strain expressing GFP under the regulation of the same CD4C regulatory sequences as in CD4C/HIV Tg mice (Figure 4B) was generated. Mice from five CD4C/GFP Tg founder reporter mouse lines expressed GFP in the same cell populations [notably in immature and mature $CD4^+$ (and to a lesser extent $CD8^+$) T cells and in cells of the macrophage/dendritic lineage] (Supplemental Figure S3), as those previously documented to express several transgenes under the control of the same CD4C regulatory elements.[27,32,41,76,77] This includes expression in $CD8^+$ T cells, although such expression was much lower with human *CD4* than with *GFP* reporter gene. This may be biologically relevant. Indeed, human $CD8^+$ T cells expressing CD4 have been described,[78,79] and infection of peripheral $CD8^+$ T cells has been reported in human AIDS and found to correlate with depletion of $CD8^+$ T cells.[80–82]

Interestingly, GFP expression was also detectable in kidney glomeruli of Tg mice from all five founder lines analyzed (Figure 4C), indicating that this glomerular expression was independent of the transgene integration site. Interestingly, high GFP expression was heterogeneous between and within glomeruli (Figure 4, D–I), suggesting a focal and segmental distribution. Few of the glomerular GFP-positive cells were positive for WT-1 and synaptopodin, and some were positive for factor VIII (von Willebrand factor) and CD31 (Figure4, J–N), markers of podocytes and endothelial cells, respectively. However, a large proportion were positive for α8 integrin (Figure 4O), a marker specific in glomeruli for mesangial cells.[83] Quantification of colocalization signals on kidney sections (Figure 4P) revealed higher expression in mesangial cells and in a larger proportion of them. Higher and preferential expression of surrogate genes in mesangial cells of CD4C/GFP Tg mice was confirmed by FACS analysis (Figure 4Q) and in purified cytospotted GFP-positive glomerular cells (Figure 5, A–C) as well as in two additional Tg reporter mouse strains harboring the same CD4C regulatory elements [namely, the inducible [CD4C/rtTA × tetracycline operon (tetO)/GFP] Tg mice expressing GFP[41] (Figure 5, D–G) and the CD4C/HIV-mutant H (MutH) Tg mice faithfully expressing all *HIV-1* genes except *nef*[28] (Figure 5H)]. Together, these results indicate that the CD4C regulatory elements are preferentially active in mesangial cells of kidney glomeruli and in a smaller proportion, and at lower levels, of glomerular endothelial and epithelial (podocyte) cells.

The levels of GFP expression in the glomerular cells were compared relative to $CD4^+$ T cells of CD4C/GFP and (CD4C/rtTA × tetO/GFP) Tg mice by FACS analysis. These levels, reflected in values of mean fluorescence intensity (MFI), were lower in glomerular mesangial (approximately 2.5- to 10-fold, respectively) and endothelial (approximately 10-fold) cells than in peripheral $CD4^+$ T cells (Supplemental Figure S4), suggesting that low Nef expression in specific kidney cell subset(s) is sufficient to induce severe kidney damage.

Tg Mesangial Cells Are Proliferating

In the early phase of the disease, microscopic examination indicated focal minimal mesangial hypercellularity in the less affected Tg glomeruli, progressing to diffuse mild mesangial hypercellularity and mesangial matrix expansion, as the disease advanced (Figures 1I, 3H, and 6A). Staining of mesangial cells with α8 integrin, a mesangial cell-specific marker,[83] indicated patchy and nodular distribution of Tg mesangial cells, in contrast to their tree-like arrangement in non-Tg cells (Figure 6, B and C). Electron microscopy showed that Tg mesangial cells were also hypertrophic (Figure 6, E and F) and mildly hyperplastic (Figure 6E) relative to non-Tg ones (Figure 6D).

Tg GFP reporter mice were used to assess the proliferation of glomerular GFP-positive cells, largely representing

Figure 5 Preferential expression of surrogate genes [green fluorescent protein (GFP), inducible GFP, and HIV Gag p24] in glomerular mesangial cells through the regulatory sequences (CD4C) of the human *CD4* gene. **A–C:** Identification of glomerular GFP-positive cells from CD4C/GFP transgenic (Tg) mice. Cells were obtained from purified glomeruli, further digested, fixed, and cytospotted onto glass slides before staining with antibody against α8 integrin, synaptopodin (Synapto), and CD31. Fluorescence analysis of labeled antibody (Ab) and endogenous GFP was performed by confocal microscopy on 700 to 800 cells. **A:** Representative images of GFP positivity and staining with the indicated Ab (**top panels**) or with their isotype controls (Ctrls; **bottom panels**). **B:** Percentage of GFP-positive glomerular cells of total glomerular cells purified (total) or belonging to each cell subset [mesangial cells ($\alpha8$ integrin$^+$), podocytes (synaptopodin$^+$), or endothelial cells ($CD31^+$)] of GFP-positive cells counted. **C:** Quantification of GFP fluorescence intensity in each glomerular cell subset. Data expressed as sum of mean GFP intensity (pixels). **D–G:** Kidney glomerular cell expression through the CD4C promoter in inducible double [CD4C/reverse tetracyclin transactivator (rtTA) × tetracycline operon (tetO)/GFP] Tg mice. **D:** GFP positivity in kidney tissue sections. Note that most GFP^{High} cells are in glomeruli. The dotted appearance of GFP-positive cells reflects expression of GFP in nuclei in this reporter strain. **E–G:** Purified glomerular cells were stained with the same Ab and analyzed by confocal microscopy after being cytospotted (**E** and **F**), as above and by fluorescence-activated cell sorting (**G**). **E–G:** GFP colocalization with cell-specific markers was evaluated and tabulated as percentage on 700 to 800 cells (**E**) and sum of mean GFP intensity (pixels; **F**) or mean fluorescence intensity (MFI; **G**). Data from two experiments with four mice. **H:** Kidney glomerular cell expression through the CD4C promoter in CD4C/HIV-MutH Tg mice. Purified glomerular cytospotted cells were stained with anti-gag p24 Ab and with each of the same cell-specific Ab used in **A**. Gag p24 colocalization with cell-specific markers was tabulated as percentage on 700 to 800 cells, as above. Note that mesangial cells represent most GFP- or p24-positive cells with the highest GFP intensity. Data from four (CD4C/GFP) and two (CD4C/rtTA × tetO/GFP) experiments with 10 and 4 mice, respectively. $^*P < 0.05$, $^{**}P < 0.01$, $^{***}P < 0.001$, and $^{****}P < 0.0001$. Original magnification: ×40 (**A**); ×10 (**D**). AF, Alexa Fluor.

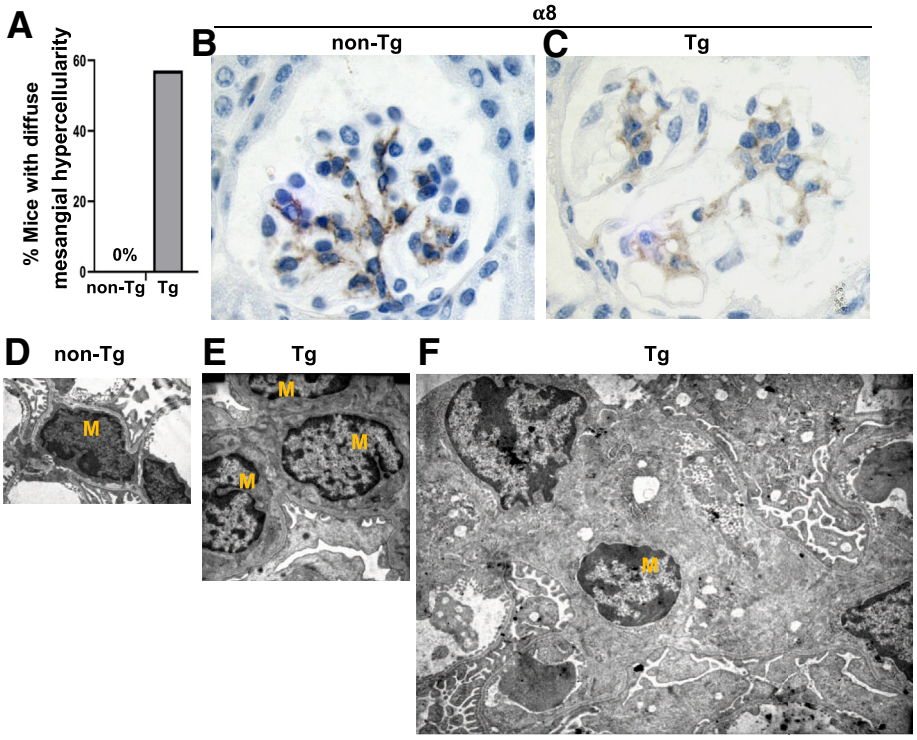

Figure 6 Mesangial cell expansion in CD4C/HIV-Nef transgenic (Tg) mice. **A:** Light microscopic assessment of mesangial cells in 30 to 40 glomeruli per kidney in seven Tg and four non-Tg kidneys. Mesangial hypercellularity is defined as three or more cells per mesangial area. Diffuse: ≥50% glomeruli affected. Graph shows the percentage of Tg (4/7, 57.1%) and non-Tg (0/4, 0%) mice with diffuse mesangial cell hyperplasia. **B** and **C:** Immunohistochemistry was performed on kidney sections with antibodies against α8 integrin (five non-Tg and five Tg mice). **A** and **B:** Note a fainter labeling around nodular structure of Tg mesangial cells (**B**), compare with the tree-like staining in normal non-Tg mice (**A**). **D**–**F:** Electron microscopy on the same tissues as those shown in Figure 3, G through N. **D**–**F:** Mice were 40 (**D** and **E**) or 54 (**F**) days old. **D**–**F:** Tg mesangial cells are hyperplastic (**E**) and enlarged (**E** and **F**). Original magnification: ×100 (**B** and **C**); ×10,000 (**D**–**F**). M, mesangial cells.

mesangial cells (Figures 4O and 5). This analysis was done with BrdU-fed (CD4C/GFP × CD4C/HIV-Nef) double Tg mice. A significant proportion (approximately 35%) of BrdU-positive kidney glomerular cells ($n = 245$) were GFP-positive cells, suggesting that mesangial (and possibly endothelial) cells are proliferating in Nef Tg mice.

The CD4C Regulatory Elements Are Active in Subsets of Extraglomerular Kidney Cells

Extraglomerular cells, including cells of the renin lineage, can be the progenitors of podocytes, mesangial cells, and parietal cells in disease conditions.[84–86] Herein, CD4C/GFP reporter mice were used to investigate extraglomerular GFP expression. Small clusters of GFP^+ SMA^+ (Figure 7, A–C) or platelet-derived growth factor receptor-β $(PDGFR\beta)^+$ (Figure 7, D and E) cells were found around some glomeruli, in the paraglomerular areas, sometimes at the vascular pole of glomeruli. They may represent smooth muscle cells of the juxtaglomerular apparatus and/or extraglomerular mesangial cells or mesangial cell precursors, the latter known to be located in these structures.[84,87] However, renin-positive cells did not seem to express GFP (Figure 7, D and E). Less frequently, GFP^+ $PDGFR\beta^+$ cells were also detected in peritubular areas (Figure 7, F–H). They are likely to represent smooth muscle cells lining the vasculature.

However, GFP expression was largely absent in Src-suppressed protein kinase C substrate–positive parietal cells (Figure 7I). Interestingly, staining of Src-suppressed protein kinase C substrate–positive parietal cells with CD44 (an activation marker) was strong in double (CD4C/GFP × CD4C/Nef) Tg kidneys (Figure 7K), but hardly detectable in single CD4C/GFP Tg kidneys (Figure 7J). Together, these results indicate that parietal cells are activated in these Nef Tg mice, and suggest that this activation is indirect, as these cells do not appear to express GFP (Nef).

Tg Glomerular Cells, including Mesangial Cells, Show Enhanced Plating Efficiency and Proliferation *in Vitro* and Reduced Transgene Expression

To determine whether Tg glomerular cells show abnormalities in tissue culture, glomeruli from Tg and non-Tg mice were purified (Figure 7L) and plated in Petri dishes *in vitro*. The exit and/or growth of cells from Nef Tg glomeruli was faster than that of non-Tg glomeruli (Figure 7M). Nef Tg cells produced increased stress fibers, detected with phalloidin (Figure 7, N and O).

Interestingly, while working with purified CD4C/GFP Tg glomeruli incubated *in vitro*, a rapid loss of GFP fluorescence intensity was noticed once mesangial/endothelial cells had attached to the dish, from 125 ± 45 at day 5 compared with 43 ± 12 at day 10. This suggests that the CD4C promoter is rapidly down-regulated during attachment and growth of mesangial/endothelial cells *in vitro*, a phenomenon that may explain the discordant results obtained by infecting cultured human mesangial cells with HIV-1.[88–92]

Strong Influence of Host Genetic Factors on the Development of HIVAN in CD4C/Nef Tg Mice

To determine whether the mouse background influences the severity of kidney disease, C3H/HeNHsd CD4C/Nef Tg mice were further bred as heterozygous for at least six generations on different backgrounds, before being studied for survival (reflecting severity of kidney disease) and kidney morphology. A large proportion of Tg mice of four strains (DBA/2, 129/J, CBA/J, and FVB/NJ) died within 4.5 months of age (Supplemental Table S2), and had severe kidney disease (scores >3.5). FVB/NJ Tg mice were the most susceptible, as 44.6% (21/47) died within 1 month of age, compared with <13% for the other three strains. In contrast, A/J Tg mice were the least susceptible, as only 1 of 47 (2%) died within 4.5 months of age (Supplemental Table S2); among those assessed ($n = 11$), only minimal kidney lesions were detected (scores = 0.2), strongly suggesting the presence of resistant gene(s) to kidney disease in this strain, thus providing valuable information to begin the relevant breedings required to possibly identify the gene(s) conferring such resistance. The other assessed Tg strains (BALB/c, C3H/HeNHsd, C57BL/6, C58/J, and SWR/J) showed intermediate survival (Supplemental Table S2) and kidney lesions (scores 2 to 3). These results indicate that the development of kidney disease in CD4C/Nef Tg mice is much influenced by host gene(s) yet to be identified. These genes are unlikely to all represent those influencing severity of kidney disease in FVB/N Tg26 Tg mice, because (FVB × BALB/c)F_1 Tg26 mice develop no renal disease,[93] whereas BALB/c and FVB/NJ CD4C/Nef Tg mice do.

Src, but Not *Fyn*, *Hck/Fgr*, *Lck*, or *Lyn*, Deletion Ameliorates Kidney Morphology in CD4C/HIV Tg Mice without Improving Albuminuria

The mechanism by which Nef expression leads to kidney disease is unknown. In other cell types, Nef was reported to activate Src-related kinases, in particular Lck,[94] Src, and Hck.[95] To assess the contribution of these effectors to kidney disease development, CD4C/HIV Tg mice were bred on backgrounds deficient for a few Src-related genes. *Hck* deletion is known to not improve much kidney disease of CD4C/HIV Tg mice.[31] Similarly, moderate to severe kidney disease was present in most *Fyn*-, *Hck/Fgr*-, *Lck*-, or *Lyn*-deficient CD4C/HIV Tg mice and was not significantly different from that of control heterozygote Tg mice (Supplemental Table S1). In contrast, most *Src*-deficient Tg mice showed less severe macroscopic (Supplemental Figure S5) and microscopic (Figure 8, A and B) kidney disease, with significantly lower desmin (Figure 8, C and D) and SMA (Figure 8E) glomerular staining than in control wild-type or heterozygous Tg mice. However, albuminuria was not significantly different in $Src^{-/-}$ or $Src^{+/-}$ Tg mice (Figure 8F). In particular, some $Src^{-/-}$ Tg mice with few histologic signs of kidney damage still showed high albuminuria. These results indicate that some kidney dysfunction persists in absence of *Src* and suggest segregation of two distinct phenotypes (namely, tubular cyst formation and glomerular damage).

Because activated Src augments nitric oxide production in mesangial cells,[96] the effect of *Nos2* or *Nos3* deletion was evaluated on kidney disease of CD4C/HIV Tg mice. Homozygous (−/−) CD4C/Nef or $CD4CHIV^{MutA}$ Tg mice bred on *Nos2* or *Nos3* gene-deficient background, respectively, still develop severe kidney disease comparable to that of heterozygous (+/−) or wild-type Tg mice (Supplemental Table S1).

HIVAN Is Less Severe in CD4C/HIV Tg Mice Deleted of *Hck/Lyn*

Mortality (reflecting kidney disease) is delayed in CD4C/HIV Tg mice harboring a deletion of *Hck*,[31] suggesting a possible role of Hck in the development of Nef-induced kidney disease. Because compensation by *Lyn* occurs in absence of *Hck*,[59] HIV Tg mice were bred on double *Hck/Lyn* gene-deficient background. Because $Hck^{-/-}/Lyn^{-/-}$ mice die within 2 months from lung inflammation,[97] kidneys of all groups of mice were assessed earlier (at 4 to 9 weeks). Most $Hck^{-/-}/Lyn^{-/-}$ *nef* Tg triple-mutant mice showed much less severe histologic signs of kidney disease than heterozygote $Hck^{+/-}/Lyn^{+/-}$, $Hck^{+/-}/Lyn^{-/-}$, $Hck^{+/-}/Lyn^{+/+}$, $Hck^{-/-}/Lyn^{+/-}$, and $Hck^{-/-}/Lyn^{+/+}$ Tg littermates, most of which developed severe kidney disease (Figure 8G). This was confirmed by significant decrease of desmin (Figure 8H) and SMA (Figure 8I) staining. In addition, albuminuria was normalized in most $Hck^{-/-}/Lyn^{-/-}$ *nef* Tg mice (Figure 8J), indicating an improvement of kidney function. These results indicate that Hck and Lyn are required for optimal Nef signalization inducing HIVAN.

Discussion

Nef-Induced Mouse Kidney Disease, Dependent on Kidney Parenchymal Cells Permissive for Human *CD4* Gene Expression

Only *nef* is necessary and sufficient to induce the development of kidney disease in the CD4C/HIV Tg mouse model studied here, characterized by *nef* expression beginning early in life.[28] A similar and undistinguishable kidney disease also

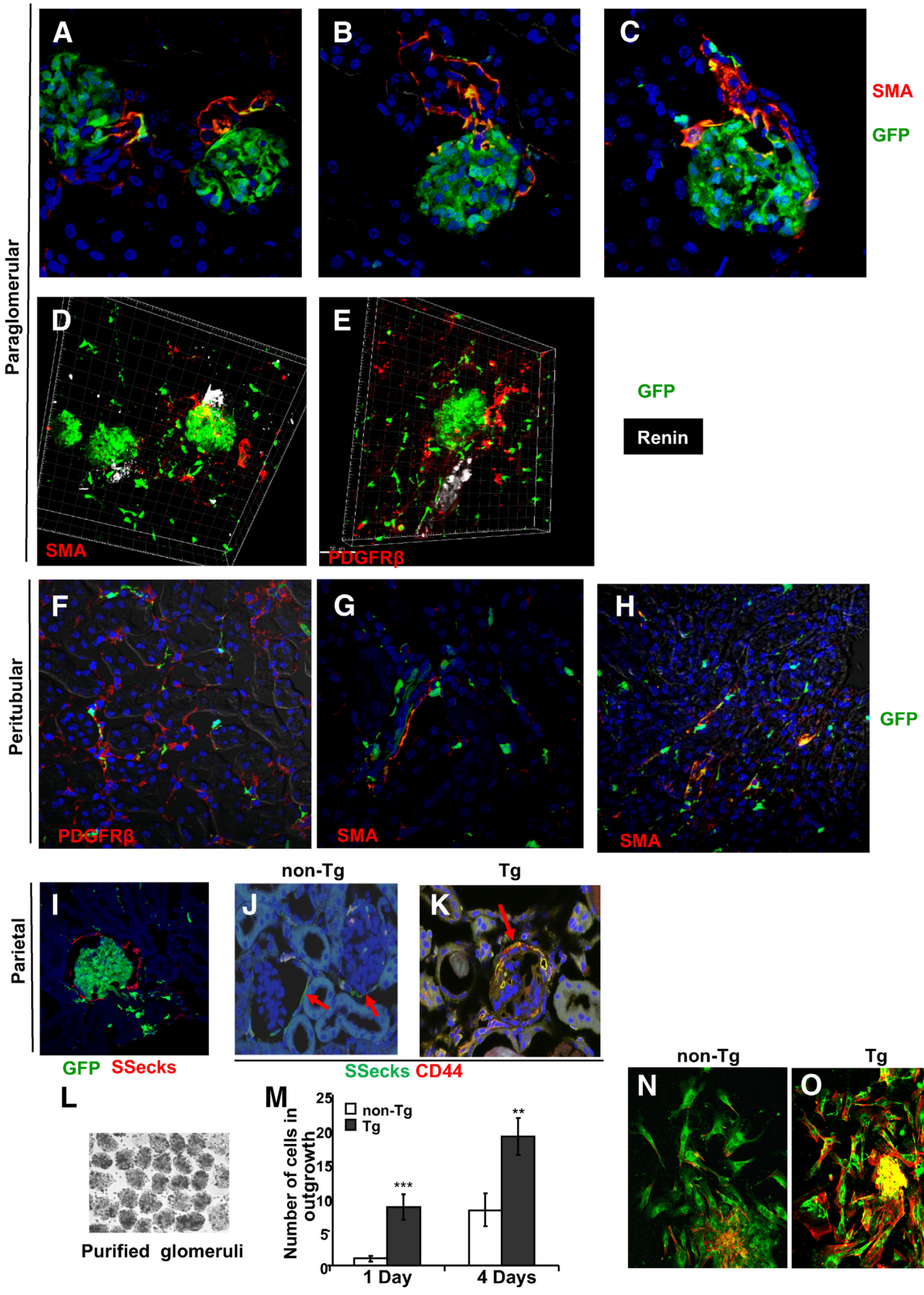
Paraglomerular
A
B
C
SMA
GFP
D
E
SMA
PDGFRβ
GFP
Renin
Peritubular
F
G
H
PDGFRβ
SMA
SMA
GFP
Parietal
non-Tg
Tg
I
J
K
GFP SSecks
SSecks CD44
L
Purified glomeruli
M
Number of cells in outgrowth
non-Tg
Tg
***
**
1 Day
4 Days
non-Tg
Tg
N
O

develops following inducible expression of *nef* during adulthood, through the same CD4C regulatory elements.[41] Indeed, no other *HIV* gene is capable of inducing kidney disease when expressed by the CD4C promoter, as shown in CD4C/HIV^{MutH} Tg mice expressing all HIV genes, except *nef*.[28] This represents an important characteristic distinguishing this model from others exhibiting nephropathy following *vpr* expression.[26,98–100] These contrasting results strongly suggest that the cell subset(s) in which the CD4C promoter is active and which is(are) critical for the development of kidney disease in CD4C/Nef Tg mice, is (are) different from that (those) expressing *vpr* in other models.

Herein, several experiments were designed to identify the Nef-expressing cell population(s) involved in kidney disease. Previous studies have shown that Nef expression in CD4$^+$ T cells, macrophages, or dendritic cells, or transplantation of Tg fetal liver hematopoietic cells, does not elicit kidney disease[34] and that CD4$^+$ T cells are not required for its development.[35] Herein, these results were extended to show that the presence of all T and B cells is dispensable for the development of kidney disease in these Tg mice. These results led to the hypothesis that expression of Nef in kidney parenchymal rather than hematopoietic cells may contribute to kidney injury in this model.

Studies with reporter mice confirmed this hypothesis. Indeed, the regulatory sequences of the human *CD4* gene (CD4C) were shown to drive faithful expression of surrogate genes, such as *HIV-1*, human *CD4*, and *GFP*, not only in CD4$^+$ T cells, myeloid cells,[27,28,32,76] and osteoclasts,[30] as expected, but also in kidney cells, mainly in glomeruli. In these latter cells, high expression was predominantly found in mesangial cells, whereas fewer endothelial cells and podocytes expressed at lower levels. This pattern of expression of the CD4C regulatory elements was observed in several independent Tg lines, ruling out an effect of the transgene integration site and suggesting that these Tg lines represent genuine reporter strains reflecting faithful expression of the human CD4 gene.

CD4C-mediated expression in glomerular mesangial and endothelial cells may reflect their possible origin from a common precursor.[101] This result is consistent with the detectable expression of CD4 in human mesangial cells[92] or glomerular cells morphologically similar to mesangial cells[102] and with the infectibility of glomerular mesangial[89,91,92] and endothelial[89] cells by HIV *in vitro*. Also, the fact that CD4C promoter activity is rapidly down-regulated in cultured Tg mesangial cells may explain the discordant results regarding HIV-1 infection of human mesangial cells *in vitro*,[88–92] because infection of human cells by HIV-1 largely occurs through the CD4 receptor. Together, these results suggest that mesangial cells have the potential to be infected by HIV-1 and to induce kidney damage when expressing Nef.

HIVAN in CD4C/Nef Tg Mice

The question remains whether the kidney disease in CD4C/Nef Tg mice is a model for human HIVAN. Generating an animal model of HIVAN is challenging because not much is known about human HIVAN. CD4C/Nef Tg mice were generated based on the assumption that the cells involved in the development of kidney disease would express human CD4, the major receptor for HIV-1 infection. As any mouse model of kidney disease, these Nef Tg mice have obvious limitations: i) HIV may infect human kidney glomerular cells through a different receptor than CD4, thus making human CD4-mediated Nef expression possibly less relevant; ii) HIV is not replicating, and no immune response against HIV is elicited; iii) also, only one HIV gene, *nef,* is expressed at young age, in a much larger number of target cells; and iv) in addition, *APOL1*, an important modifier gene for human HIVAN, is absent in mice.[103] Therefore, its influence cannot be investigated unless these CD4C/Nef Tg mice are crossed with already available Tg mice harboring different human *APOL1* alleles,[104–106] specifically comparing the reference allele (*G0*) with the risk-conferring alleles (*G1* or *G2*) in double (CD4C/Nef × *APOL1*) Tg mice.

Despite these limitations, the current data indicate that the kidney disease of CD4C/HIV Tg mice shows characteristics of human HIVAN. It represents a collapsing form of FSGS associated with interstitial nephritis and microcystic tubular dilatation. It also shares other features with human HIVAN, such as modest proliferation of podocytes and mesangial

Figure 7 The CD4C regulatory elements are active in subsets of extraglomerular cells, but not in parietal cells, and Nef expression through these CD4C elements leads to enhanced glomerular cell outgrowth *in vitro*. **A**–**I:** Activity of CD4C in extraglomerular cells. **A**–**H:** Confocal immunofluorescence of kidney sections from CD4C/green fluorescent protein (GFP) transgenic (Tg) mice showing GFP-positive paraglomerular (**A**–**E**) or peritubular (**F**–**H**) structures stained with the indicated antibody [Ab; anti–smooth muscle actin (SMA), anti–platelet-derived growth factor receptor-β (PDGFRβ; red), or anti-renin (white) Ab] and with Alexa Fluor–labeled secondary Ab. Note colocalization in some cells within these structures. **I:** Staining of parietal cells with anti–Src-suppressed protein kinase C substrate (SSecks) Ab (red). Few cells show colocalization with endogenous GFP. **J** and **K:** Activation of parietal cells studied with CD44, an activation marker for parietal cells. Representative image of costaining of kidney sections from non-Tg and CD4C/Nef Tg mice with sheep anti-SSecks/anti-sheep Alexa-488 and rat anti-CD44/anti-rat Alexa 568 Ab. Note stronger signal of both markers in Tg cells. Colocalization is observed in Tg cells, but not in non-Tg cells. Images were acquired with confocal 710 microscope in Z-stack mode. **Arrows**: immune-positive parietal cells. **L**–**O:** *In vitro* growth of glomerular cells. **L:** Purified kidney glomeruli from non-Tg and CD4C/Nef Tg mice were incubated in Petri dishes (approximately 1500 glomeruli/dish). **M:** Adherent cells around glomeruli were counted after 1 and 4 days in culture. Representative experiment of four performed. In the three other experiments, the *P* values were <0.03, <0.01, and 0.0004. **N** and **O:** Attached non-Tg (**N**) and Tg (**O**) cells were labeled with phalloidin (green) and anti-fibronectin (red). Note increased staining of Nef Tg cells. $n = 3$ non-Tg mice (**J** and **K**); $n = 4$ CD4C/Nef Tg mice (**J** and **K**). $^{**}P < 0.01$, $^{***}P < 0.001$. Original magnification: ×40 (**A**–**K**); ×100 (**N** and **O**).

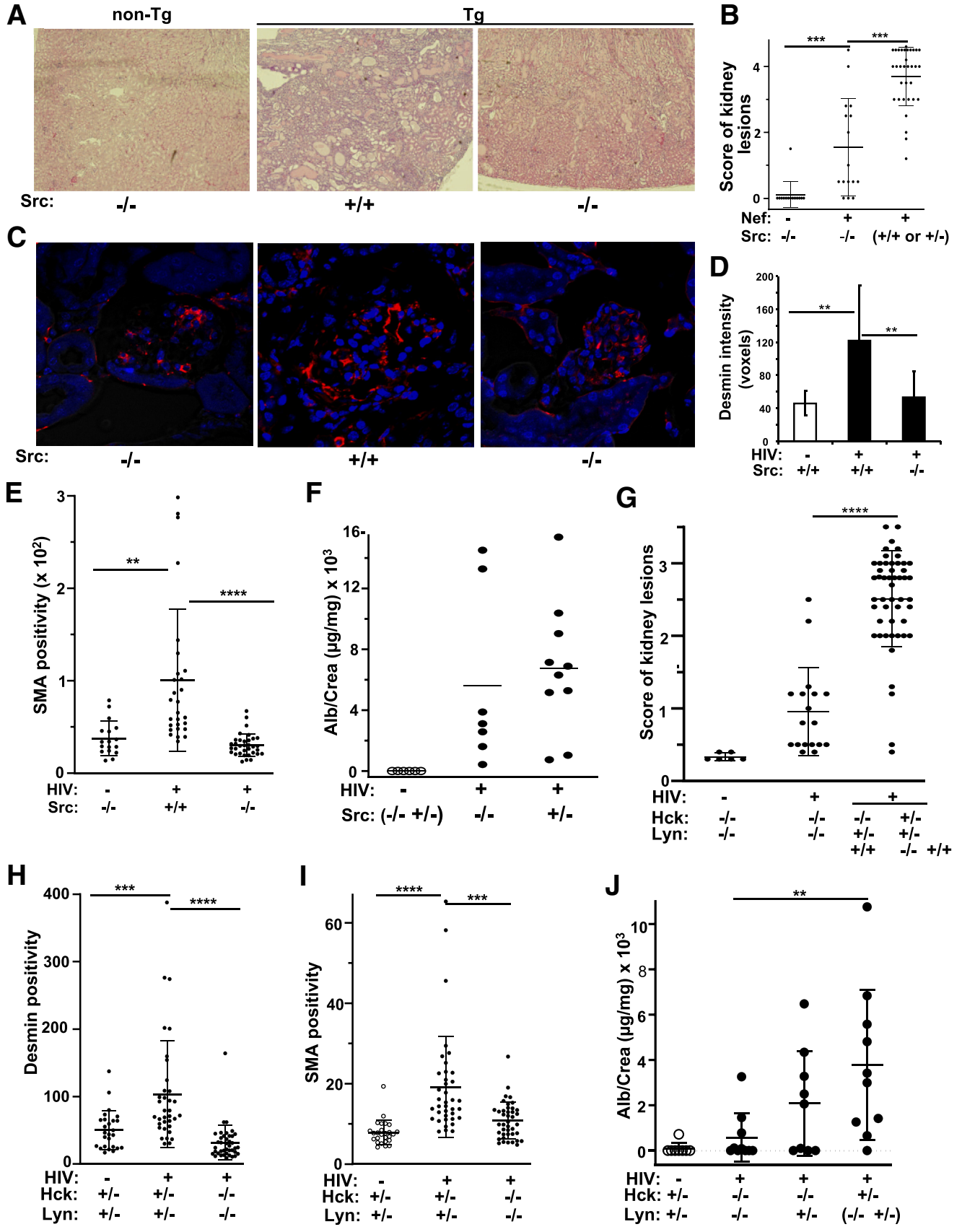
A
non-Tg
Tg
Src: -/- +/+ -/-
B
Score of kidney lesions
Nef: - + +
Src: -/- -/- (+/+ or +/-)
C
Src: -/- +/+ -/-
D
Desmin intensity (voxels)
HIV: - + +
Src: +/+ +/+ -/-
E
SMA positivity (x 10²)
HIV: - + +
Src: -/- +/+ -/-
F
Alb/Crea (µg/mg) x 10³
HIV: - + +
Src: (-/- +/-) -/- +/-
G
Score of kidney lesions
HIV: - + +
Hck: -/- -/- -/- +/-
Lyn: -/- -/- +/- +/-
+/+ -/- +/+
H
Desmin positivity
HIV: - + +
Hck: +/- +/- -/-
Lyn: +/- +/- -/-
I
SMA positivity
HIV: - + +
Hck: +/- +/- -/-
Lyn: +/- +/- -/-
J
Alb/Crea (µg/mg) x 10³
HIV: - + + +
Hck: +/- -/- -/- +/-
Lyn: +/- -/- +/- (-/- +/-)

cells, high proliferation of tubular and parietal cells, down-regulation of podocyte markers,[1] and acquisition of CK18 positivity by parietal cells.[10,11] The presence of modest mesangial cell expansion, especially observed in human pediatric HIVAN,[107] likely reflects early Nef expression in these Tg mice.

It has been proposed that the proliferating glomerular cells in human and animal models of HIVAN represent podocytes, based on their morphologic characteristics.[6,7,9,24] Herein, a podocyte hypercellularity in CD4C/Nef Tg mice was observed, although proliferation of podocytes themselves, assessed by BrdU incorporation, was modest. In fact, a significant fraction of proliferating glomerular cells in human HIVAN represents migrating proliferating parietal cells.[10,11] The current data are consistent with these latter studies. Indeed, among proliferating glomerular cells, a high percentage (approximately 45%) were identified as parietal cells. In addition, parietal Tg cells were found to be activated (CK18 and CD44 positive) and to be present within glomeruli. Thus, the kidney disease in CD4C/Nef Tg mice shows many similarities with human HIVAN.

A Role for Nef-Expressing Mesangial Cells in Initiating HIVAN

Expression of Nef in CD4C/Nef Tg mice occurred in different parenchymal glomerular cell subsets: at low levels in a few podocytes and endothelial cells and at higher levels in a large proportion of mesangial cells. At least one of these Nef-expressing cell subsets is likely to initiate glomerular lesions.

The low CD4C-mediated expression detected in a small proportion of podocytes may contribute to glomerular lesions. However, experimental evidence suggests that this may not be a major pathway of disease. First, expression of *nef* alone in podocytes of Tg mice is insufficient to induce all features of HIVAN.[25,26] Second, kidney disease failed to develop when *nef* was expressed with other *HIV* genes in podocytes of Tg mice,[108] although another study indicated severe FSGS in such Tg mice.[26,109] These conflicting results are thought to be related to levels of Nef achieved in podocytes, and it was hypothesized that high Nef levels are needed to damage podocytes.[26,108] These findings suggest that the low levels of Nef (GFP) detected in a small fraction of CD4C/Nef Tg podocytes may not be sufficient to cause major podocyte injury. Consistent with this interpretation, expression of Nef was seen in cells permissive to CD4C regulatory elements, at levels fourfold to fivefold lower (in founders F21380, F26622, and F27011) than in founder F27367 used in the present work, still led to severe kidney disease and death within 6 months of age,[28] suggesting that the CD4C-targetted cell subset, likely mesangial cells, is more susceptible to the effects of low concentration of Nef than podocytes. Third, genetic data also support the notion that the Nef-expressing cell subset involved in the development of kidney glomerular disease in CD4C/Nef Tg mice is distinct from podocytes. Indeed, in nephrotic syndrome-1 (Nphs1)/Nef10 Tg mice, expressing *nef* alone in podocytes, the severity of kidney pathology was similar whether mice were bred on C57BL/6 or FVB/N background.[26] In contrast, kidney disease of CD4C/Nef Tg mice was significantly more severe when Tg mice were bred on FVB/N than on C57BL/6 background. Fourth, among all *HIV* genes expressed through the CD4C regulatory elements, only *nef*, even at low levels, can induce HIVAN.[28] In contrast, *vpr* expression in podocytes of Tg mice induces kidney pathology,[26,99,100] again strongly suggesting that the CD4C promoter is active in a cell subset distinct from podocytes and driving disease development. These cumulative results all point in the same direction and strongly suggest that glomerular kidney disease in CD4C/Nef Tg mice is unlikely to be only driven by the low expression of Nef in a small proportion of podocytes.

The current data suggest that mesangial cells may be involved in the development of Tg HIVAN. They represent most of the glomerular cells expressing Nef, and the cell subset expressing it most abundantly. Moreover, their pattern of expression (focal and segmental) is reminiscent of the distribution of the FSGS lesions themselves, suggesting that the latter reflect the presence of mesangial cells expressing higher Nef levels focally and segmentally. Thus, glomerular lesions, including podocyte injury/loss in CD4C/Nef Tg mice, may to be triggered by bystander Nef-expressing mesangial cells. The use of a Nef-expressing mesangial-specific promoter (not yet available) would be helpful to further validate this notion.

Figure 8 Deletion of *Src* partially and that of *Hck/Lyn* largely abrogates renal pathology of CD4C/HIV-Nef transgenic (Tg) mice. **A**–**J:** CD4C/HIV^{MutA} or CD4C/HIV-Nef Tg mice were bred on *Src* (**A**–**F**) or *Hck/Lyn* (**G**–**J**) gene-deficient background, respectively, and assessed for HIV-1–associated nephropathy at the age of 5 to 8 or 1 to 2.25 months, respectively. **A:** Hematoxylin and eosin staining of kidneys from representative *Src*-deficient Tg mice. **B** and **G:** Evaluation of microscopic pathology in kidneys of *Src* (**B**) or *Hck/Lyn* (**G**) gene-deficient Tg mice. **C**, **D**, and **H:** Quantification of desmin-positive areas in glomeruli of *Src* (**C** and **D**) or *Hck/Lyn* (**H**) gene-deficient Tg mice. **E** and **I:** Quantification of smooth muscle actin (SMA) positivity, expressed as mean of voxel counts, in glomeruli of *Src* (**E**) or *Hck/Lyn* (**I**) gene-deficient Tg mice. **F** and **J:** Albuminuria in *Src* (**F**) or *Hck/Lyn* (**J**) gene-deficient Tg mice. Ratios of albumin (Alb)/creatinine (Crea) concentration were measured. Data for desmin and SMA staining were obtained by confocal microscopy. **B**, **F**, **G**, and **J:** In graphs showing scores (**B** and **G**) and albumin levels (**F** and **J**), each dot represents a mouse. **D**, **E**, **H**, and **I:** In graphs showing levels of marker staining, each dot represents one glomerulus from three to four mice per group. Statistical analysis was performed using unpaired *t*-test and nested analysis of variance. Note that SMA and desmin stainings were more variable in +/− or +/+ Tg than in −/− Tg or non-Tg glomeruli, as documented in the more dispersed values of immunoreactive positivity. $^{**}P < 0.01$, $^{***}P < 0.001$, and $^{****}P < 0.0001$. Original magnification: ×5 (**A**); ×40 (**C**).

However, it is possible that expression of Nef in glomerular mesangial cells may not be sufficient to elicit the full spectrum of renal pathologic changes in CD4C/Nef Tg mice. First, the few endothelial cells expressing Nef at low levels may participate in these changes. The generation of Tg mice showing restricted expression of *nef* in endothelial cells would be required to assess the contribution of endothelial cells in the development of FSGS. Second, the periglomerular GFP (Nef)−expressing cells found to be SMA positive may contribute to glomerular pathology alone or with mesangial cells. Third, it is tempting to suggest that the observed Nef-expressing PDGFRβ$^+$ smooth muscle cells in the peritubular vasculature may participate in the formation of tubular cysts. These cells share many features with mesangial cells,[87] and smooth muscle cells have been reported to contribute to HIV podocyte injury *in vitro*.[110] The involvement of this distinct cell subset in the formation of cysts, but possibly not in the development of glomerular lesions, would be compatible with the observed segregation of these two phenotypes in *Src* knockout CD4C/HIV Tg mice (Figure 8, A−F).

Cellular Pathogenesis of HIVAN in CD4C/Nef Tg Mice: A Bystander Effect on Podocytes

By showing that HIVAN in CD4C/HIV Tg mice is associated with Nef expression mainly in other kidney cells than podocytes, we propose an alternative model of cellular pathogenesis, whereby bystander Nef-expressing glomerular cells, most of those identified in this model as being mesangial cells, cause major damage to other cell subsets, themselves apparently not or poorly expressing Nef. This appears to be the case for podocytes that are injured, most showing no or low GFP (Nef) expression. Also, most epithelial parietal cells do not express GFP (Nef) but constitute a significant proportion of proliferating Tg kidney cells. They are activated, showing increased CK18 and CD44 positivity and being among the first to exhibit enhanced SMA and desmin immunoreactivity, and they seem to migrate within the glomeruli. Interestingly, in human HIVAN, most proliferating glomerular cells were identified as parietal cells, often acquiring CK8 positivity,[10,11] suggesting that kidney disease of the CD4C/HIV-Nef mice reflects this important feature of human HIVAN. Similarly, tubular cyst formation arises in absence of detectable GFP (Nef) expression in epithelial tubular cells of Tg mice, by an apparent indirect mechanism, possibly from bystander Nef-expressing PDGFRβ$^+$ smooth muscle cells of the peritubular vessels. In SIV-infected macaques, the development of tubular microcystic dilatation also appears to be indirect, occurring in absence of SIV expression in tubular cells.[3,5] Future work should identify the putative paracrine effectors, likely either overproduced by or downregulated in Nef-expressing kidney cells, and whose modulated levels may alter and/or damage epithelial glomerular and tubular cells.

Involvement of Src Family Members in HIVAN Development

The molecular basis for the development of HIVAN is likely to be complex and to involve genes active in different types of kidney cells. To identify key processes of Tg HIVAN, CD4C/HIV Tg mice were bred on backgrounds deleted of candidate genes involved in important pathways, such apoptosis (*Bax*, *Trp53*, *Tnf*, *Tnfrsf1b*, and *Tnfsf10*), chemokine signaling (*Ccl2*, *Ccl3*, *Ccr2*, *Ccr5*, and *Cx3cr1*), and cytokine signaling (*Ifng* and *Il6*)[76] or NO production (*Nos3* and *Nos2*). Some of these pathways have previously been thought to be involved in HIVAN[90,111,112] or in other forms of nephropathy.[70,71,74,75,113] The current studies showed that none of these genes is required for the development of kidney disease in CD4C/Nef Tg mice, thus ruling out several critical candidates and pathways.

More proximal candidate effectors were explored, those binding to Nef, in particular members of the Src kinase family.[95] Deletion of *Src* was found to improve morphology of Tg kidneys, although it did not prevent albuminuria. This result indicates that these two phenotypes can be segregated and suggests that their development requires distinct effectors, possibly expressed in distinct cell subsets, as discussed above. Future studies with cell-specific deletion of *Src*, in particular glomerular or tubular cell subset, could be instrumental in understanding the partial protection of Src from kidney disease in CD4C/Nef Tg mice.

Interestingly, deletion of *Hck/Lyn* was found to be protective against kidney pathology, consistent with the absence of kidney disease in our CD4C/Nef^{AxxAxxQ} Tg mice expressing Nef mutated in its proline-rich domain,[31] required for binding to Hck.[95] Together, these data suggest a Nef-Hck/Lyn interaction in Nef-expressing mesangial cells, and possibly in PDGFRβ-positive cells. We propose that this interaction represents a proximal event for the development of HIVAN. Nef most probably activates Hck/Lyn in kidney cells, as it does in other cell types,[95] including in spleen cells of our CD11c/Nef Tg mice.[33] The critical role of Hck/Lyn and Src in the development of all or some of the phenotypes of HIVAN is of clinical interest, as these protein kinases represent excellent targets for drug treatment.

Conclusions

The CD4C/GFP Tg mice described here represent a reporter (readout) strain for the expression of the human *CD4* gene. In fact, human mesangial cells have been shown to express CD4 and be infectable by HIV *in vitro*.[89−92] We propose that they may become infected in human individuals. If this happens, the development of HIVAN would most likely be caused by Nef and occur through similar cellular and molecular pathways as in the CD4C/Nef Tg model, considering that the three critical signaling molecules (Hck/Lyn and Src) identified here are well conserved between mouse and human.

Acknowledgments

We thank Philip Murphy (NIH) (CX3CR-1), Barrett J. Rollins (Dana-Farber Cancer Institute) (monocyte chemoattractant protein-1), Don Cook (University of North Carolina) (macrophage inflammatory protein-1α), Tak Mak (University of Toronto) (CD8), William A. Kuziel (University of North Carolina) (CCR-2 and CCR-5), Bernard Malissen (INSERM—Centre National de la Recherche Scientifique—University of Marseille) (CD3ϵ), Foo Y. Liew (University of Glasgow) (inducible nitric oxide synthase), and Kristi Phalmer (Amgen) (TRAIL), for providing the indicated gene-deficient mouse lines; Walter Schurch (Centre Hospitalier de l'Université de Montréal/Hôtel-Dieu Hospital, Montreal, ON, Canada) for helpful discussions; Dominic Filion (Microscopy and Imaging Core), Louis Gaboury (University of Montreal), and Virginie Calderon (Bioinformatics Core) for assistance in microscopy analysis, immunohistochemistry, and statistical analysis, respectively; Ginette Massé, Benoît Laganière, Audrey-Ann Kustec, Lin Gia, Stéphanie Lemay, Karina Lamarre, Marie-Eve Higgins, Eve-Lyne Thivierge, Jean-René Sylvestre, and Isabelle Corbin for excellent technical assistance; and Eric Massicotte, Julie Lord, and Martine Dupuis (Flow Cytometry Core) and Dominique Lauzière, Annie Lavallée, and Simone Terouz (Histology Core) for help with cell sorting/fluorescence-activated cell sorting and for cutting tissue sections, respectively.

Author Contributions

E.P., C.H., M.C., P.C., N.B., and C.F. performed experiments and acquired and analyzed data; Z.H. analyzed results, designed transgene DNA constructs, and supervised their construction; E.P., C.H., P.C., and Z.H. developed the project and edited the manuscript; C.A.L. provided Fgr, Hck, and Lyn gene-deficient strains; S.B. provided anti-Nef sd19 VHH DNA clone; C.H. and V.R. analyzed kidney sections by light and electron microscopes and wrote pathologic description; and P.J. designed studies, coordinated experiments, analyzed data, and wrote the manuscript.

Supplemental Data

Supplemental material for this article can be found at *http://doi.org/10.1016/j.ajpath.2023.02.006*.

References

1. D'Agati V, Appel GB: Renal pathology of human immunodeficiency virus infection. Semin Nephrol 1998, 18:406—421
2. Ross MJ, Klotman PE: HIV-associated nephropathy. AIDS 2004, 18: 1089—1099
3. Alpers CE, Tsai CC, Hudkins KL, Cui Y, Kuller L, Benveniste RE, Ward JM, Morton WR: Focal segmental glomerulosclerosis in primates infected with a simian immunodeficiency virus. Aids Res Hum Retrovir 1997, 13:413—424
4. Gattone VH, Tian C, Zhuge W, Sahni M, Narayan O, Stephens EB: SIV-associated nephropathy in rhesus macaques infected with lymphocyte-tropic SIVmac239. AIDS Res Hum Retroviruses 1998, 14:1163—1180
5. Stephens EB, Tian C, Li Z, Narayan O, Gattone VH 2nd: Rhesus macaques infected with macrophage-tropic simian immunodeficiency virus (SIVmacR71/17E) exhibit extensive focal segmental and global glomerulosclerosis. J Virol 1998, 72:8820—8832
6. Barisoni L, Kriz W, Mundel P, D'Agati V: The dysregulated podocyte phenotype: a novel concept in the pathogenesis of collapsing idiopathic focal segmental glomerulosclerosis and HIV-associated nephropathy. J Am Soc Nephrol 1999, 10:51—61
7. Barisoni L, Mokrzycki M, Sablay L, Nagata M, Yamase H, Mundel P: Podocyte cell cycle regulation and proliferation in collapsing glomerulopathies. Kidney Int 2000, 58:137—143
8. Bruggeman LA, Ross MD, Tanji N, Cara A, Dikman S, Gordon RE, Burns GC, D'Agati VD, Winston JA, Klotman ME, Klotman PE: Renal epithelium is a previously unrecognized site of HIV-1 infection. J Am Soc Nephrol 2000, 11:2079—2087
9. He JC, Husain M, Sunamoto M, D'Agati VD, Klotman ME, Iyengar R, Klotman PE: Nef stimulates proliferation of glomerular podocytes through activation of Src-dependent Stat3 and MAPK1,2 pathways. J Clin Invest 2004, 114:643—651
10. Dijkman HB, Weening JJ, Smeets B, Verrijp KC, van Kuppevelt TH, Assmann KK, Steenbergen EJ, Wetzels JF: Proliferating cells in HIV and pamidronate-associated collapsing focal segmental glomerulosclerosis are parietal epithelial cells. Kidney Int 2006, 70:338—344
11. Smeets B, Dijkman HB, Wetzels JF, Steenbergen EJ: Lessons from studies on focal segmental glomerulosclerosis: an important role for parietal epithelial cells? J Pathol 2006, 210:263—272
12. Barbiano dB, Genderini A, Vago L, Parravicini C, Bertoli S, Landriani N: Absence of HIV antigens in renal tissue from patients with HIV-associated nephropathy. Nephrol Dial Transplant 1990, 5: 489—492
13. Nadasdy T, Hanson-Painton O, Davis LD, Miller KW, DeBault LE, Burns DK, Silva FG: Conditions affecting the immunohistochemical detection of HIV in fixed and embedded renal and nonrenal tissues. Mod Pathol 1992, 5:283—291
14. Cohen AH, Sun NC, Shapshak P, Imagawa DT: Demonstration of human immunodeficiency virus in renal epithelium in HIV-associated nephropathy. Mod Pathol 1989, 2:125—128
15. Kimmel PL, Ferreira-Centeno A, Farkas-Szallasi T, Abraham AA, Garrett CT: Viral DNA in microdissected renal biopsy tissue from HIV infected patients with nephrotic syndrome. Kidney Int 1993, 43: 1347—1352
16. Ross MJ, Bruggeman LA, Wilson PD, Klotman PE: Microcyst formation and HIV-1 gene expression occur in multiple nephron segments in HIV-associated nephropathy. J Am Soc Nephrol 2001, 12: 2645—2651
17. Winston JA, Bruggeman LA, Ross MD, Jacobson J, Ross L, D'Agati VD, Klotman PE, Klotman ME: Nephropathy and establishment of a renal reservoir of HIV type 1 during primary infection. N Engl J Med 2001, 344:1979—1984
18. Marras D, Bruggeman LA, Gao F, Tanji N, Mansukhani MM, Cara A, Ross MD, Gusella GL, Benson G, D'Agati VD, Hahn BH, Klotman ME, Klotman PE: Replication and compartmentalization of HIV-1 in kidney epithelium of patients with HIV-associated nephropathy. Nat Med 2002, 8:522—526
19. Canaud G, Dejucq-Rainsford N, Avettand-Fenoel V, Viard JP, Anglicheau D, Bienaime F, Muorah M, Galmiche L, Gribouval O, Noel LH, Satie AP, Martinez F, Sberro-Soussan R, Scemla A, Gubler MC, Friedlander G, Antignac C, Timsit MO, Onetti MA, Terzi F, Rouzioux C, Legendre C: The kidney as a reservoir for HIV-1 after renal transplantation. J Am Soc Nephrol 2014, 25: 407—419

20. Bruggeman LA, Dikman S, Meng C, Quaggin SE, Coffman TM, Klotman PE: Nephropathy in human immunodeficiency virus-1 transgenic mice is due to renal transgene expression. J Clin Invest 1997, 100:84−92
21. Barisoni L, Bruggeman LA, Mundel P, D'Agati VD, Klotman PE: HIV-1 induces renal epithelial dedifferentiation in a transgenic model of HIV-associated nephropathy. Kidney Int 2000, 58: 173−181
22. Dickie P, Felser J, Eckhaus M, Bryant J, Silver J, Marinos N, Notkins AL: HIV-associated nephropathy in transgenic mice expressing HIV-1 genes. Virology 1991, 185:109−119
23. Klotman PE, Notkins AL: Transgenic models of human immunodeficiency virus type-1. Curr Top Microbiol Immunol 1996, 206:197−222
24. Nelson PJ, Sunamoto M, Husain M, Gelman IH: HIV-1 expression induces cyclin D1 expression and pRb phosphorylation in infected podocytes: cell-cycle mechanisms contributing to the proliferative phenotype in HIV-associated nephropathy. BMC Microbiol 2002, 2: 26−33
25. Husain M, D'Agati VD, He JC, Klotman ME, Klotman PE: HIV-1 Nef induces dedifferentiation of podocytes in vivo: a characteristic feature of HIVAN. AIDS 2005, 19:1975−1980
26. Zuo Y, Matsusaka T, Zhong J, Ma J, Ma LJ, Hanna Z, Jolicoeur P, Fogo AB, Ichikawa I: HIV-1 genes vpr and nef synergistically damage podocytes, leading to glomerulosclerosis. J Am Soc Nephrol 2006, 17:2832−2843
27. Hanna Z, Kay DG, Cool M, Jothy S, Rebai N, Jolicoeur P: Transgenic mice expressing human immunodeficiency virus type 1 in immune cells develop a severe AIDS-like disease. J Virol 1998, 72: 121−132
28. Hanna Z, Kay DG, Rebai N, Guimond A, Jothy S, Jolicoeur P: Nef harbors a major determinant of pathogenicity for an AIDS-like disease induced by HIV-1 in transgenic mice. Cell 1998, 95:163−175
29. Kay DG, Yue P, Hanna Z, Jothy S, Tremblay E, Jolicoeur P: Cardiac disease in transgenic mice expressing human immunodeficiency virus-1 Nef in cells of the immune system. Am J Pathol 2002, 161: 321−335
30. Raynaud-Messina B, Bracq L, Dupont M, Souriant S, Usmani SM, Proag A, Pingris K, Soldan V, Thibault C, Capilla F, Al ST, Gennero I, Jurdic P, Jolicoeur P, Davignon JL, Mempel TR, Benichou S, Maridonneau-Parini I, Verollet C: Bone degradation machinery of osteoclasts: an HIV-1 target that contributes to bone loss. Proc Natl Acad Sci U S A 2018, 115:E2556−E2565
31. Hanna Z, Weng X, Kay DG, Poudrier J, Lowell C, Jolicoeur P: The pathogenicity of human immunodeficiency virus (HIV) type 1 Nef in CD4C/HIV transgenic mice is abolished by mutation of its SH3-binding domain, and disease development is delayed in the absence of Hck. J Virol 2001, 75:9378−9392
32. Hanna Z, Rebai N, Poudrier J, Jolicoeur P: Distinct regulatory elements are required for faithful expression of human CD4 in T-cells, macrophages and dendritic cells of transgenic mice. Blood 2001, 98: 2275−2278
33. Priceputu E, Cool M, Bouchard N, Caceres-Cortes JR, Lowell CA, Hanna Z, Jolicoeur P: HIV-1 Nef induces Hck/Lyn-dependent expansion of myeloid-derived suppressor cells associated with elevated interleukin-17/G-CSF Levels. J Virol 2021, 95:e0047121
34. Hanna Z, Priceputu E, Chrobak P, Hu C, Dugas V, Goupil M, Marquis M, de Repentigny L, Jolicoeur P: Selective expression of human immunodeficiency virus Nef in specific immune cell populations of transgenic mice is associated with distinct AIDS-like phenotypes. J Virol 2009, 83:9743−9758
35. Weng X, Priceputu E, Chrobak P, Poudrier J, Kay DG, Hanna Z, Mak TW, Jolicoeur P: CD4 T cells from CD4C/HIV nef transgenic mice show enhanced activation in vivo with impaired proliferation in vitro, but are dispensable for the development of a severe AIDS-like organ disease. J Virol 2004, 78:5244−5257
36. Hanna Z, Priceputu E, Kay DG, Poudrier J, Chrobak P, Jolicoeur P: In vivo mutational analysis of the N-terminal region of HIV-1 Nef reveals critical motifs for the development of an AIDS-like disease in CD4C/HIV transgenic mice. Virology 2004, 327:273−286
37. Hanna Z, Priceputu E, Hu C, Vincent P, Jolicoeur P: HIV-1 Nef mutations abrogating downregulation of CD4 affect other Nef functions and show reduced pathogenicity in transgenic mice. Virology 2006, 346:40−52
38. Vincent P, Priceputu E, Kay D, Saksela K, Jolicoeur P, Hanna Z: Activation of p21-activated kinase 2 and its association with Nef are conserved in murine cells but are not sufficient to induce an AIDS-like disease in CD4C/HIV transgenic mice. J Biol Chem 2006, 281:6940−6954
39. Priceputu E, Hanna Z, Hu C, Simard M-C, Vincent P, Wildum S, Schindler M, Kirchhoff F, Jolicoeur P: Primary human immunodeficiency virus type 1 nef alleles show major differences in pathogenicity in transgenic mice. J Virol 2007, 81:4677−4693
40. Chrobak P, Afkhami S, Priceputu E, Poudrier J, Meunier C, Hanna Z, Sparwasser T, Jolicoeur P: 162-HIV Nef expression favors the accumulation of CD4+ Treg cells which retain some important suppressive functions. J Immunol 2014, 192:1681−1692
41. Rahim MM, Chrobak P, Hu C, Hanna Z, Jolicoeur P: Adult AIDS-like disease in a novel inducible human immunodeficiency virus type 1 Nef transgenic mouse model: CD4+ T-cell activation is Nef dependent and can occur in the absence of lymphophenia. J Virol 2009, 83:11830−11846
42. Fung-Leung WP, Schilham MW, Rahemtulla A, Kundig TM, Vollenweider M, Potter J, van Ewijk W, Mak TW: CD8 is needed for development of cytotoxic T cells but not helper T cells. Cell 1991, 65: 443−449
43. Kitamura D, Roes J, Kuhn R, Rajewsky K: A B cell-deficient mouse by targeted disruption of the membrane exon of the immunoglobulin mu chain gene. Nature 1991, 350:423−426
44. Malissen M, Gillet A, Ardouin L, Bouvier G, Trucy J, Ferrier P, Vivier E, Malissen B: Altered T cell development in mice with a targeted mutation of the CD3-e gene. EMBO J 1995, 14: 4641−4653
45. Gu H, Zou YR, Rajewsky K: Independent control of immunoglobulin switch recombination at individual switch regions evidenced through Cre-loxP-mediated gene targeting. Cell 1993, 73:1155−1164
46. Cook DN, Beck MA, Coffman TM, Kirby SL, Sheridan JF, Pragnell IBS O: Requirement of MIP-1 alpha for an inflammatory response to viral infection. Science 1995, 269:1583−1585
47. Lu B, Rutledge BJ, Gu L, Fiorillo J, Lukacs NW, Kunkel SL, North R, Gerard C, Rollins BJ: Abnormalities in monocyte recruitment and cytokine expression in monocyte chemoattractant protein 1-deficient mice. J Exp Med 1998, 187:601−608
48. Kuziel WA, Morgan SJ, Dawson TC, Griffin S, Smithies O, Ley K, Maeda N: Severe reduction in leukocyte adhesion and monocyte extravasation in mice deficient in CC chemokine receptor 2. Proc Natl Acad Sci U S A 1997, 94:12053−12058
49. Tran EH, Kuziel WA, Owens T: Induction of experimental autoimmune encephalomyelitis in C57BL/6 mice deficient in either the chemokine macrophage inflammatory protein-1alpha or its CCR5 receptor. Eur J Immunol 2000, 30:1410−1415
50. Combadiere C, Potteaux S, Gao JL, Esposito B, Casanova S, Lee EJ, Debre P, Tedgui A, Murphy PM, Mallat Z: Decreased atherosclerotic lesion formation in CX3CR1/apolipoprotein E double knockout mice. Circulation 2003, 107:1009−1016
51. Knudson CM, Tung KS, Tourtellotte WG, Brown GA, Korsmeyer SJ: Bax-deficient mice with lymphoid hyperplasia and male germ cell death. Science 1995, 270:96−99
52. Jacks T, Remington L, Williams BO, Schmitt EM, Halachmi S, Bronson RT, Weinberg RA: Tumor spectrum analysis in p53-mutant mice. Curr Biol 1994, 4:1−7
53. Pasparakis M, Alexopoulou L, Episkopou V, Kollias G: Immune and inflammatory responses in TNF alpha-deficient mice: a critical requirement for TNF alpha in the formation of primary B cell follicles, follicular dendritic cell networks and germinal centers, and in the

maturation of the humoral immune response. J Exp Med 1996, 184: 1397−1411
54. Erickson SL, de Sauvage FJ, Kikly K, Carver-Moore K, Pitts-Meek SG N, Sheehan KC, Schreiber RD, Goeddel DV, Moore MW: Decreased sensitivity to tumour-necrosis factor but normal T- cell development in TNF receptor-2-deficient mice. Nature 1994, 372: 560−563
55. Sedger LM, Glaccum MB, Schuh JC, Kanaly ST, Williamson E, Kayagaki N, Yun T, Smolak P, Le T, Goodwin R, Gliniak B: Characterization of the in vivo function of TNF-alpha-related apoptosis-inducing ligand, TRAIL/Apo2L, using TRAIL/Apo2L gene-deficient mice. Eur J Immunol 2002, 32:2246−2254
56. Shesely EG, Maeda N, Kim HS, Desai KM, Krege JH, Laubach VE, Sherman PA, Sessa WC, Smithies O: Elevated blood pressures in mice lacking endothelial nitric oxide synthase. Proc Natl Acad Sci U S A 1996, 93:13176−13181
57. Wei XQ, Charles IG, Smith A, Ure J, Feng GJ, Huang FP, Xu D, MullerW, Moncada S, Liew FY: Altered immune responses in mice lacking inducible nitric oxide synthase. Nature 1995, 375:408−411
58. Stein PL, Lee HM, Rich S, Soriano P: pp59fyn Mutant mice display differential signaling in thymocytes and peripheral T cells. Cell 1992, 70:741−750
59. Lowell CA, Soriano P, Varmus HE: Functional overlap in the src gene family: inactivation of hck and fgr impairs natural immunity. Genes Dev 1994, 8:387−398
60. Chan VW, Meng F, Soriano P, DeFranco AL, Lowell CA: Characterization of the B lymphocyte populations in Lyn- deficient mice and the role of Lyn in signal initiation and down-regulation. Immunity 1997, 7:69−81
61. Soriano P, Montgomery C, Geske R, Bradley A: Targeted disruption of the c-src proto-oncogene leads to osteopetrosis in mice. Cell 1991, 64:693−702
62. Molina TJ, Kishihara K, Siderovski DP, van Ewijk W, Narendran A, Timms E, Wakeham A, Paige CJ, Hartmann KU, Veillette A: Profound block in thymocyte development in mice lacking p56lck. Nature 1992, 357:161−164
63. Simard M-C, Chrobak P, Kay DG, Hanna Z, Jothy S, Jolicoeur P: Expression of simian immunodeficiency virus nef in immune cells of transgenic mice leads to a severe AIDS-like disease. J Virol 2002, 76: 3981−3995
64. Takemoto M, Asker N, Gerhardt H, Lundkvist A, Johansson BR, Saito Y, Betsholtz C: A new method for large scale isolation of kidney glomeruli from mice. Am J Pathol 2002, 161:799−805
65. Hu C, Dievart A, Lupien M, Calvo E, Tremblay G, Jolicoeur P: Overexpression of activated murine Notch1 and Notch3 in transgenic mice blocks mammary gland development and induces mammary tumors. Am J Pathol 2006, 168:973−990
66. Heckmann A, Waltzinger C, Jolicoeur P, Dreano M, Kosco-Vilbois MH, Sagot Y: IKK2 inhibitor alleviates kidney and wasting diseases in a murine model of human AIDS. Am J Pathol 2004, 164:1253−1262
67. Djudjaj S, Papasotiriou M, Bülow RD, Wagnerova A, Lindenmeyer MT, Cohen CD, Strnad P, Goumenos DS, Floege J, Boor P: Keratins are novel markers of renal epithelial cell injury. Kidney Int 2016, 89:792−808
68. Priceputu E, Rodrigue I, Chrobak P, Poudrier J, Mak TW, Hanna Z, Hu C, Kay DG, Jolicoeur P: The Nef-mediated AIDS-like disease of CD4C/HIV transgenic mice is associated with increased Fas/FasL expression on T cells and T cell death, but is not prevented in Fas, FasL, TNFR-1 and ICE deficient nor in Bcl2-expressing transgenic mice. J Virol 2005, 79:6377−6391
69. Kim EY, Roshanravan H, Dryer SE: Changes in podocyte TRPC channels evoked by plasma and sera from patients with recurrent FSGS and by putative glomerular permeability factors. Biochim Biophys Acta Mol Basis Dis 2017, 1863:2342−2354
70. Pedigo CE, Ducasa GM, Leclercq F, Sloan A, Mitrofanova A, Hashmi T, Molina-David J, Ge M, Lassenius MI, Forsblom C, Lehto M, Groop PH, Kretzler M, Eddy S, Martini S, Reich H, Wahl P, Ghiggeri G, Faul C, Burke GW 3rd, Kretz O, Huber TB, Mendez AJ, Merscher S, Fornoni A: Local TNF causes NFATc1-dependent cholesterol-mediated podocyte injury. J Clin Invest 2016, 126:3336−3350
71. Otalora L, Chavez E, Watford D, Tueros L, Correa M, Nair V, Ruiz P, Wahl P, Eddy S, Martini S, Kretzler M, Burke GW 3rd, Fornoni A, Merscher S: Identification of glomerular and podocyte-specific genes and pathways activated by sera of patients with focal segmental glomerulosclerosis. PLoS One 2019, 14:e0222948
72. Hu S, Han R, Shi J, Zhu X, Qin W, Zeng C, Bao H, Liu Z: The long noncoding RNA LOC105374325 causes podocyte injury in individuals with focal segmental glomerulosclerosis. J Biol Chem 2018, 293:20227−20239
73. Bouchet J, Basmaciogullari SE, Chrobak P, Stolp B, Bouchard N, Fackler OT, Chames P, Jolicoeur P, Benichou S, Baty D: Inhibition of the Nef regulatory protein of HIV-1 by a single domain antibody. Blood 2011, 117:3559−3568
74. Besbas N, Kalyoncu M, Cil O, Ozgul RK, Bakkaloglu A, Ozaltin F: MCP1 2518 A/G polymorphism affects progression of childhood focal segmental glomerulosclerosis. Ren Fail 2015, 37:1435−1439
75. Wilkening A, Krappe J, Mühe AM, Lindenmeyer MT, Eltrich N, Luckow B, Vielhauer V: C-C chemokine receptor type 2 mediates glomerular injury and interstitial fibrosis in focal segmental glomerulosclerosis. Nephrol Dial Transplant 2020, 35:227−239
76. Poudrier J, Weng X, Kay DG, Paré G, Calvo EL, Hanna Z, Kosco-Vilbois MH, Jolicoeur P: The AIDS disease of CD4C/HIV transgenic mice shows impaired germinal centers and autoantibodies and develops in the absence of IFN-g and IL-6. Immunity 2001, 15:173−185
77. Hanna Z, Simard C, Jolicoeur P: Specific expression of the human CD4 gene in mature CD4+CD8- and immature CD4+CD8+T cells, and in macrophages of transgenic mice. Mol Cell Biol 1994, 14: 1084−1094
78. Clénet ML, Gagnon F, Moratalla AC, Viel EC, Arbour N: Peripheral human CD4(+)CD8(+) T lymphocytes exhibit a memory phenotype and enhanced responses to IL-2, IL-7 and IL-15. Sci Rep 2017, 7: 11612
79. Overgaard NH, Jung JW, Steptoe RJ, Wells JW: CD4+/CD8+ double-positive T cells: more than just a developmental stage? J Leukoc Biol 2015, 97:31−38
80. Livingstone WJ, Moore M, Innes D, Bell JE, Simmonds P: Frequent infection of peripheral blood CD8-positive T-lymphocytes with HIV-1: Edinburgh Heterosexual Transmission Study Group. Lancet 1996, 348:649−654
81. Saha K, Zhang J, Zerhouni B: Evidence of productively infected CD8+ T cells in patients with AIDS: implications for HIV-1 pathogenesis. J Acquir Immune Defic Syndr 2001, 26:199−207
82. Cochrane A, Imlach S, Leen C, Scott G, Kennedy D, Simmonds P: High levels of human immunodeficiency virus infection of CD8 lymphocytes expressing CD4 in vivo. J Virol 2004, 78:9862−9871
83. Hartner A, Schocklmann H, Prols F, Muller U, Sterzel RB: Alpha8 integrin in glomerular mesangial cells and in experimental glomerulonephritis. Kidney Int 1999, 56:1468−1480
84. Hugo C, Shankland SJ, Bowen-Pope DF, Couser WG, Johnson RJ: Extraglomerular origin of the mesangial cell after injury: a new role of the juxtaglomerular apparatus. J Clin Invest 1997, 100: 786−794
85. Pippin JW, Sparks MA, Glenn ST, Buitrago S, Coffman TM, Duffield JS, Gross KW, Shankland SJ: Cells of renin lineage are progenitors of podocytes and parietal epithelial cells in experimental glomerular disease. Am J Pathol 2013, 183:542−557
86. Starke C, Betz H, Hickmann L, Lachmann P, Neubauer B, Kopp JB, Sequeira-Lopez ML, Gomez RA, Hohenstein B, Todorov VT, Hugo CP: Renin lineage cells repopulate the glomerular mesangium after injury. J Am Soc Nephrol 2014, 26:48−54
87. Shaw I, Rider S, Mullins J, Hughes J, Péault B: Pericytes in the renal vasculature: roles in health and disease. Nat Rev Nephrol 2018, 14: 521−534

88. Alpers CE, McClure J, Bursten SL: Human mesangial cells are resistant to productive infection by multiple strains of human immunodeficiency virus types 1 and 2. Am J Kidney Dis 1992, 19: 126−130
89. Green DF, Resnick L, Bourgoignie JJ: HIV infects glomerular endothelial and mesangial but not epithelial cells in vitro. Kidney Int 1992, 41:956−960
90. Conaldi PG, Biancone L, Bottelli A, Wade-Evans A, Racusen LC, Boccellino M, Orlandi V, Serra C, Camussi G, Toniolo A: HIV-1 kills renal tubular epithelial cells in vitro by triggering an apoptotic pathway involving caspase activation and Fas upregulation. J Clin Invest 1998, 102:2041−2049
91. Tokizawa S, Shimizu N, Hui-Yu L, Deyu F, Haraguchi Y, Oite T, Hoshino H: Infection of mesangial cells with HIV and SIV: identification of GPR1 as a coreceptor. Kidney Int 2000, 58:607−617
92. Conaldi PG, Bottelli A, Wade-Evans A, Biancone L, Baj A, Cantaluppi V, Serra C, Dolei A, Toniolo A, Camussi G: HIV-persistent infection and cytokine induction in mesangial cells: a potential mechanism for HIV-associated glomerulosclerosis. AIDS 2000, 14:2045−2047
93. Gharavi AG, Ahmad T, Wong RD, Hooshyar R, Vaughn J, Oller S, Frankel RZ, Bruggeman LA, D'Agati VD, Klotman PE, Lifton RP: Mapping a locus for susceptibility to HIV-1-associated nephropathy to mouse chromosome 3. Proc Natl Acad Sci U S A 2004, 101: 2488−2493
94. Chrobak P, Simard MC, Bouchard N, Ndolo TM, Guertin J, Hanna Z, Dave V, Jolicoeur P: HIV-1 Nef disrupts maturation of CD4+ T cells through CD4/lck modulation. J Immunol 2010, 185:3948−3959
95. Trible RP, Emert-Sedlak L, Smithgall TE: HIV-1 Nef selectively activates Src family kinases Hck, Lyn, and c-Src through direct SH3 domain interaction. J Biol Chem 2006, 281:27029−27038
96. Jalal DI, Kone BC: Src activation of NF-kappaB augments IL-1beta-induced nitric oxide production in mesangial cells. J Am Soc Nephrol 2006, 17:99−106
97. Xiao W, Hong H, Kawakami Y, Lowell CA, Kawakami T: Regulation of myeloproliferation and M2 macrophage programming in mice by Lyn/Hck, SHIP, and Stat5. J Clin Invest 2008, 118: 924−934
98. Dickie P, Roberts A, Uwiera R, Witmer J, Sharma K, Kopp JB: Focal glomerulosclerosis in proviral and c-fms transgenic mice links Vpr expression to HIV-associated nephropathy. Virology 2004, 322: 69−81
99. Hiramatsu N, Hiromura K, Shigehara T, Kuroiwa T, Ideura H, Sakurai N, Takeuchi S, Tomioka M, Ikeuchi H, Kaneko Y, Ueki K, Kopp JB, Nojima Y: Angiotensin II type 1 receptor blockade inhibits the development and progression of HIV-associated nephropathy in a mouse model. J Am Soc Nephrol 2007, 18:515−527
100. Kumar D, Salhan D, Magoon S, Torri DD, Sayeneni S, Sagar A, Bandhlish A, Malhotra A, Chander PN, Singhal PC: Adverse host factors exacerbate occult HIV-associated nephropathy. Am J Pathol 2011, 179:1681−1692
101. Ricono JM, Xu YC, Arar M, Jin DC, Barnes JL, Abboud HE: Morphological insights into the origin of glomerular endothelial and mesangial cells and their precursors. J Histochem Cytochem 2003, 51:141−150
102. Karlsson-Parra A, Dimeny E, Fellstrom B, Klareskog L: HIV receptors (CD4 antigen) in normal human glomerular cells. N Engl J Med 1989, 320:741
103. Kopp JB, Nelson GW, Sampath K, Johnson RC, Genovese G, An P, Friedman D, Briggs W, Dart R, Korbet S, Mokrzycki MH, Kimmel PL, Limou S, Ahuja TS, Berns JS, Fryc J, Simon EE, Smith MC, Trachtman H, Michel DM, Schelling JR, Vlahov D, Pollak M, Winkler CA: APOL1 genetic variants in focal segmental glomerulosclerosis and HIV-associated nephropathy. J Am Soc Nephrol 2011, 22:2129−2137
104. Beckerman P, Bi-Karchin J, Park AS, Qiu C, Dummer PD, Soomro I, Boustany-Kari CM, Pullen SS, Miner JH, Hu CA, Rohacs T, Inoue K, Ishibe S, Saleem MA, Palmer MB, Cuervo AM, Kopp JB, Susztak K: Transgenic expression of human APOL1 risk variants in podocytes induces kidney disease in mice. Nat Med 2017, 23:429−438
105. Bruggeman LA, Wu Z, Luo L, Madhavan S, Drawz PE, Thomas DB, Barisoni L, O'Toole JF, Sedor JR: APOL1-G0 protects podocytes in a mouse model of HIV-associated nephropathy. PLoS One 2019, 14: e0224408
106. McCarthy GM, Blasio A, Donovan OG, Schaller LB, Bock-Hughes A, Magraner JM, Suh JH, Tattersfield CF, Stillman IE, Shah SS, Zsengeller ZK, Subramanian B, Friedman DJ, Pollak MR: Recessive, gain-of-function toxicity in an APOL1 BAC transgenic mouse model mirrors human APOL1 kidney disease. Dis Model Mech 2021, 14:dmm048952
107. Ray PE, Li J, Das JR, Tang P: Childhood HIV-associated nephropathy: 36 years later. Pediatr Nephrol 2021, 36:2189−2201
108. Feng J, Bao L, Wang X, Li H, Chen Y, Xiao W, Li Z, Xie L, Lu W, Jiang H, Lee K, He JC: Low expression of HIV genes in podocytes accelerates the progression of diabetic kidney disease in mice. Kidney Int 2021, 99:914−925
109. Zhong J, Zuo Y, Ma J, Fogo AB, Jolicoeur P, Ichikawa I, Matsusaka T: Expression of HIV-1 genes in podocytes alone can lead to the full spectrum of HIV-1-associated nephropathy. Kidney Int 2005, 68:1048−1060
110. Lan X, Wen H, Saleem MA, Mikulak J, Malhotra A, Skorecki K, Singhal PC: Vascular smooth muscle cells contribute to APOL1-induced podocyte injury in HIV milieu. Exp Mol Pathol 2015, 98: 491−501
111. Ross MJ, Martinka S, D'Agati VD, Bruggeman LA: NF-kappaB regulates Fas-mediated apoptosis in HIV-associated nephropathy. J Am Soc Nephrol 2005, 16:2403−2411
112. Ross MJ, Fan C, Ross MD, Chu TH, Shi Y, Kaufman L, Zhang W, Klotman ME, Klotman PE: HIV-1 infection initiates an inflammatory cascade in human renal tubular epithelial cells. J Acquir Immune Defic Syndr 2006, 42:1−11
113. Weichert W, Paliege A, Provoost AP, Bachmann S: Upregulation of juxtaglomerular NOS1 and COX-2 precedes glomerulosclerosis in fawn-hooded hypertensive rats. Am J Physiol Ren Physiol 2001, 280: F706−F714